Article

Reference genomes and fossils revise bat family phylogeny and biogeography

https://doi.org/10.1038/s41586-026-11007-3

Received: 29 January 2026

Accepted: 10 August 2026

Check for updates

Bats are extraordinary among mammals, having uniquely evolved powered flight and laryngeal echolocation, along with disease resistance, extended healthspans and the ability to hibernate[1]. However, the evolutionary history of bats and our understanding of these adaptations remain unresolved. We analysed chromosome-level, long-read genome assemblies from 103 bat species, including 42 new assemblies, representing all 21 bat families. This dataset, expanded in d scope and assembly quality, yielded a new bat phylogeny. We placed Myzopodidae as the earliest branch within Vespertilionoidea, and resolved yangochiropteran relationships, identifying Emballonuroidea and Vespertilionoidea as sister groups. Our analysis revealed a mosaic evolutionary history across bats and explained why previous phylogenetic studies were misled. Chromosomal ancestral-state reconstructions supported 26 ancestral bat chromosomes. We integrated a morphological dataset of 699 characters for 65 species, including 44 pre-Quaternary fossils and representatives of most living bat families, with neutrally evolving genomic sites. Fossilized birth–death and dispersal–extinction cladogenesis analyses showed that bats, and thus powered flight, probably originated in Europe in the late Palaeocene, refuting African and North American origins. Placement of the fossil †*Vielasia* in the oldest 'Eochiroptera' clade indicates that laryngeal echolocation predates crown-bat diversification. Total evidence dating, including the fossil taxa, significantly reduced unrepresented basal branch lengths compared with molecular-only divergence estimates. By integrating comprehensive genomic and morphological datasets, analysed using innovative methods, we resolve long-standing controversies in bat biology and provide new insights into the evolutionary history and trait diversification of bats.

With over 1,500 species, bats account for more than one-fifth of all living mammal species[2]. They are distributed globally, are predominantly nocturnal and adapted to diverse foraging niches, ranging from insectivorous, sanguivorous, carnivorous, piscivorous, frugivorous and nectarivorous species[1]. Some species are exceptionally long-lived compared with other mammals of similar body size, capable of living 8–10 times longer than expected, showing few signs of ageing or cancer[3]. Several species host a diversity of viruses without overt disease symptoms and show unique immune adaptations[4,5]. Despite having the smallest mammalian genomes (approximately 2 Gb), they harbour a diverse endogenous genomic virosphere[4,6] and many have active DNA transposons, which is exceptionally rare among mammals[7].

The acquisition and evolution of these unique traits have been the centre of heated debates, particularly in relation to the evolution of flight and echolocation. This is probably due to the difficulties in reconstructing bat evolutionary history[8–10]. Challenges have stemmed from: homoplastic and convergent molecular and morphological characters[11,12]; conflicting phylogenetic signals[13]; a paucity of chromosome-level bat genome assemblies[1,14]; rapid speciation events resulting in incomplete lineage sorting and introgression[15]; the dearth of phylogenetic methods required to handle this complexity; and a limited and fragmented fossil record[16].

Indeed, the fossil record has provided important but incomplete insights into the early bat evolution. The oldest bat fossils, dating to the early Eocene (approximately 56–52 million years ago (Ma)), have been recovered from multiple biogeographical regions including Asia, North America, Europe and Australia, and in some cases consist of well-preserved skeletons from Lagerstätten deposits[16–18]. These fossils indicate that powered flight and echolocation had evolved by this time[16–18]. However, beyond this narrow temporal window, the bat fossil record is sparse and highly fragmented, dominated by isolated dental or postcranial elements, with a substantial proportion of bat evolutionary history estimated to be missing[17–19]. As a result, fossil evidence alone has proven insufficient to resolve the geographical origin and early diversification of bats. Biogeographical inferences integrating fossils with molecular phylogenies have proposed North American[17], African[20] or Asian[21] origins, often suggesting multiple long-distance dispersal events, but these conclusions remain sensitive to methodological limitations and data incompleteness[21,22]. In parallel, sparse genomic sampling and reliance on fragmented or low-quality genome assemblies have limited robust phylogenetic inference, hindering efforts to reconstruct and better understand bat evolution.

Taxa, genomes, annotations and alignments

To overcome these problems, the Bat1K consortium was established to generate and analyse reference-quality genome assemblies from all living bat species (https://bat1k.com). Here we present phase 1 of the

A list of authors and their affiliations appears at the end of the paper.

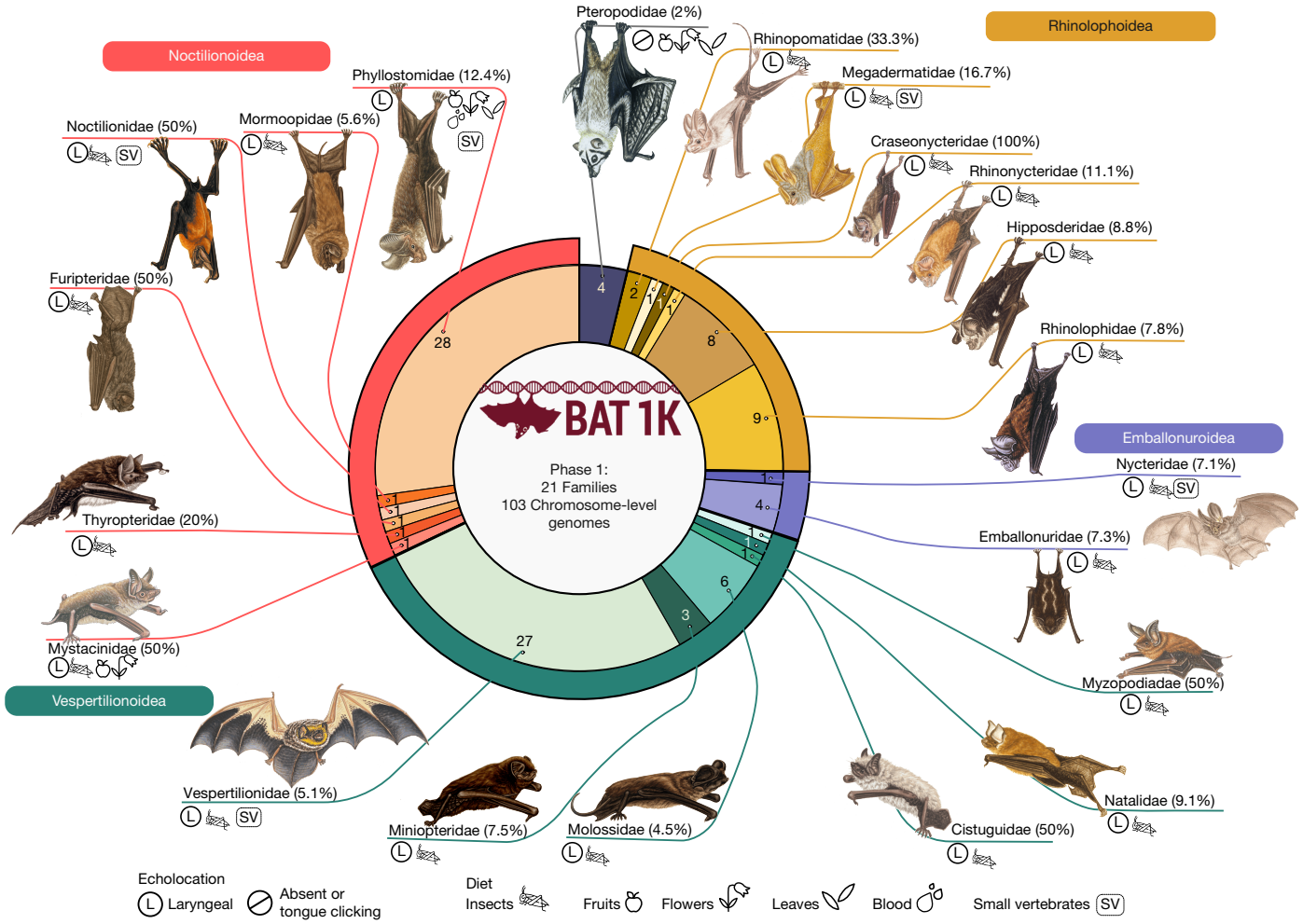

Fig. 1 | Completion of phase 1 of the Bat1K project, including 103 chromosome-level genome assemblies and annotations representing at least one species from each of the 21 currently recognized bat families. Values within each slice indicate the number of genome assemblies per family; the values adjacent to family names show species coverage (%) relative to all described species in that family. The outer colours indicate superfamilies; Myzopodidae is shown within Vespertilionoidea. The icons indicate feeding niche and echolocation capabilities in each family. Starting from the top and moving clockwise, illustrations correspond to the following families and species: Pteropodidae (*Pteropus capistratus*), Rhinopomatidae (*Rhinopoma hardwicki*), Megadermatidae (*Lavia frons*), Craseonycteridae (*Craseonycteris thonglongyai*), Rhinonycteridae (*Triaenops persicus*), Hipposideridae (*Hipposideros diadema*), Rhinolophidae (*Rhinolophus megaphyllus*), Nycteridae (*Nycteris hispida*), Emballonuridae (*Saccopteryx leptura*), Myzopodidae (*Myzopoda aurita*), Natalidae (*Natalus stramineus*), Cistugidae (*Cistugo lesueri*), Molossidae (*Eumops perotis*), Miniopteridae (*Miniopterus schreibersii*), Vespertilionidae (*Lasiurus cinereus*), Mystacinidae (*Mystacina tuberculata*), Thyropteridae (*Thyroptera tricolor*), Furipteridae (*Furipterus horrens*), Noctilionidae (*Noctilio leporinus*), Mormoopidae (*Mormoops megalophylla*) and Phyllostomidae (*Tonatia saurophila*). All illustrations were hand-drawn by Fiona Reid. The Bat1K logo was designed by Peter Lang under a Creative Commons Universal Public Domain licence CC0 1.0. Images are not drawn to scale.

project, which includes chromosome-level, long-read assemblies that represent all 21 currently recognized bat families (Fig. 1). We included members of the enigmatic families, Craseonycteridae (Thailand and Myanmar), Mystacinidae (New Zealand) and Myzopodidae (Madagascar), all regionally endemic, and the three most recently recognized bat families, Cistugidae, Rhinonycteridae and Miniopteridae[1]. Our species span deep divergences in the most species-rich bat families Phyllostomidae and Vespertilionidae, and include representatives from the families Nycteridae, Thyropteridae, Furipteridae, Noctiliionidae, Mormoopidae and Natalidae (Fig. 1, Supplementary Table 1.1 and Supplementary Note 1).

We used long-read and Hi-C sequencing to generate 42 new reference-quality chromosome-level genome assemblies representing 41 distinct species; 26 of the new genomes are haplotype-resolved assemblies (Supplementary Notes 2 and 3). The 42 new assemblies meet or exceed the key standards of Bat1K and the Earth Biogenome Project[1,23] and feature high gene completeness (Extended Data Fig. 1a–c and Supplementary Notes 4 and 5). Together with pre-existing high-quality assemblies of 62 species, our dataset comprises 103 bat species (Extended Data Fig. 1 and Supplementary Table 1.1). We also included eight outgroups from across the mammalian tree (Supplementary Note 1).

Transposable elements

Transposable elements were curated using the pipeline detailed in Supplementary Note 6 and Extended Data Fig. 1d. Thousands of novel consensus sequences were deposited in Dfam[24] (Supplementary Table 6.1; Dataset 6.1). We confirmed previous results indicating that several clades experienced extensive recent DNA transposon and rolling circle invasions while also harbouring the retrotransposons typical of most mammals[7,25], as well as the nearly complete cessation of transposable element activity in Pteropodidae[26,27].

Using heatmaps, we compared proportional transposable element accumulation across two transitional divergence periods. The first

period compares proportional transposable element accumulation in 'recent' bats (approximately18 Ma to the present) to 'early' bat lineages (approximately 18 Ma to about 46 Ma; Supplementary Fig. 6.2a). Similarly, we compared proportional transposable element accumulation in early bat lineages (approximately 18 Ma to about 46 Ma) to proportional transposable element accumulation in protobats and ancestral mammals (older than approximately 46 Ma; Supplementary Fig. 6.2b).

When comparing proportional transposable element accumulation in early bats versus their mammalian ancestors (Supplementary Fig. 6.2b), we showed that even during this early diversification, transposable elements had begun to accumulate differentially. Long interspersed nuclear elements (LINEs) increased accumulation relative to other transposable elements in miniopterids, molossids, mormoopids and phyllostomids, whereas the reverse occurred in the hipposiderids and the lineages leading to *Cistugo* and *Triaenops*. The expansion of Helitrons, exclusive to the vespertilionids[7], also began early in their history.

When comparing more recent patterns versus the early bat lineages (Supplementary Fig. 6.2a), we noticed that the cessation of LINE accumulation in the pteropodids[7,27] is accompanied by an increase in long terminal repeat accumulation. However, these are relative increases, and the lack of LINE accumulation amplifies the signal from ongoing long terminal repeat accumulation. Finally, after incorporating phylogeny, we found that transposable element accumulation is positively correlated with genome assembly size, in bats overall and within bat families ($R^2_{\text{conditional}} = 0.88$; Extended Data Fig. 2), consistent with previous analyses in mammals[7], confirming the role of transposable elements in shaping genome structure.

microRNAs

Using MirMachine[28], we identified 188 high-confidence, conserved microRNA families across all 103 bat species (Extended Data Fig. 1f and Supplementary Note 7), a sampling breath that enabled lineage-specific comparisons across the most divergent bat phylogeny to date. Although most families exhibit strong phylogenetic structure and evolutionary stability (Extended Data Fig. 3), *MIR-506*, *MIR-95*, *MIR-375* and *MIR-430* show striking copy number variation, suggesting lineage-specific expansions and regulatory diversification in bats. Given the annotation, no microRNA family losses were detected in the ancestral bat lineage (Supplementary Fig. 7.1), although we observed lineage-specific losses (for example, *MIR-675* in Pteropodidae and Noctilionoidea; and *MIR-9851* in Emballonuroidea). By contrast, families with multiple independent losses (for example, *MIR-296* and *MIR-2114*) suggest relaxed functional constraint across bat lineages (Supplementary Fig. 7.2). Together, these patterns reveal evolutionary trajectories ranging from deeply conserved families to lineage-specific expansions, clade-restricted losses and globally dispensable families.

Whole-genome alignments for phylogenomics

To leverage the high-quality assemblies for phylogenomics, we generated several whole-genome alignments. To avoid potential biases, we used two independent approaches: a reference-based strategy (MULTIZ[29]) and a reference-free method (Progressive CACTUS[30]; Supplementary Note 8). To minimize bias caused by reference species choice, we produced MULTIZ alignments for three phylogenetically informative references: *Homo sapiens* (MULTIZ *Homo* Reference (mHR)), *Myotis myotis* (mMR; Yangochiroptera) and *Rhinolophus ferrumequinum* (mRR; Yinpterochiroptera); we then compared them with corresponding CACTUS-derived projections (cHR, cMR and cRR).

MULTIZ consistently yielded higher alignment coverages than CACTUS, most likely caused by more sensitive parameter settings and the inclusion of repeat-overlapping alignments by RepeatFiller[31,32] (Extended Data Fig. 4a–c). However, both methods produced comparable and biologically consistent signals. Alignment coverage was strongly and significantly correlated with neutral branch length to the reference genome, indicating that evolutionary divergence, rather than methodological artefact, primarily explains variation in coverage across species (Extended Data Fig. 4d–f).

The phylogeny of 21 bat families

To reconstruct the evolutionary history of bats and resolve their long-standing phylogenetic controversies, we generated and analysed a comprehensive suite of genomic datasets using our 103 bat genome assemblies and eight non-bat outgroups (111 species; Supplementary Note 1). In addition to the multiple whole-genome alignments, we generated datasets of 1:1 orthologous protein-coding genes, mitochondrial genomes, neutrally evolving windows and neutral single-nucleotide polymorphisms (SNPs). We applied multiple phylogenomic inference approaches and compared the resulting topologies (Supplementary Notes 9–14). We then assessed potential systematic biases in our datasets and methods, ultimately producing a revised, genome-scale phylogeny for bats (Fig. 2). The resulting trees converged on two main topologies, which we refer to as the protein-coding gene tree (T1) and the neutral windows tree (T2), differing only by two branch rearrangements (the position of Emballonuroidea and monophyly of *Pipistrellus*; Extended Data Fig. 5). All analyses unambiguously supported the monophyly of the suborders Yinpterochiroptera and Yangochiroptera[16–18], refuting the monophyly of the echolocating lineages (Microchiroptera; Extended Data Fig. 6). Where applicable, all families were recovered as monophyletic, across all datasets and methods. We resolved long-standing phylogenetic questions regarding relationships within the Phyllostomidae (Extended Data Fig. 7) and the monophyly of *Pipistrellus* (Extended Data Fig. 8). Whole-mitochondrial analyses largely supported the nuclear phylogenies (Supplementary Note 14). However, our analyses revealed an alternative composition and branching pattern of the superfamilial groups, providing robust support for the revised placement of Myzopodidae within Vespertilionoidea, and with Emballonuroidea as sister to that group. These results call for a re-evaluation of the current-consensus bat phylogeny.

Phylogenomic position of Myzopodidae

We first analysed the protein-coding genes, using TOGA[33] to identify 1:1 orthologues (16,750 genes; Supplementary Note 9). Species trees inferred under the ASTRAL coalescent framework (Supplementary Note 9) and IQ-TREE2 maximum likelihood concatenation analyses (Supplementary Note 10) largely recapitulated previous subordinal relationships of the prevailing consensus phylogeny[6,16–18,34]. The resulting phylogenies were robust to varying levels of node support (Supplementary Note 10). They provided an alternative topology for the placement of the enigmatic family Myzopodidae (Figs. 2 and 3), the mono-generic family of sucker-footed bats endemic to Madagascar.

The placement of this family has been notoriously difficult, arguably stemming from its long branch, with different genomic regions and datasets providing conflicting support for multiple topologies[13]. Although previous studies have placed Myzopodidae within the predominantly neotropical superfamily Noctilionoidea[17], our coalescent and concatenated analysis of protein-coding genes placed Myzopodidae as the earliest branch within the panglobal superfamily Vespertilionoidea (Figs. 2 and 3). Motivated by these inconsistencies, we systematically evaluated alternative placements of Myzopodidae within Vespertilionoidea, Noctilionoidea and Emballonuroidea, or as the earliest diverging lineage within Yangochiroptera (Fig. 3a).

Across inference methods (coalescent and concatenation), protein-coding genes consistently recovered Myzopodidae (M) within Vespertilionoidea (V; Fig. 3b; coalescent and concatenated bootstrap = 100% and 100%, respectively; Extended Data Fig. 5, Supplementary Fig. 10.1

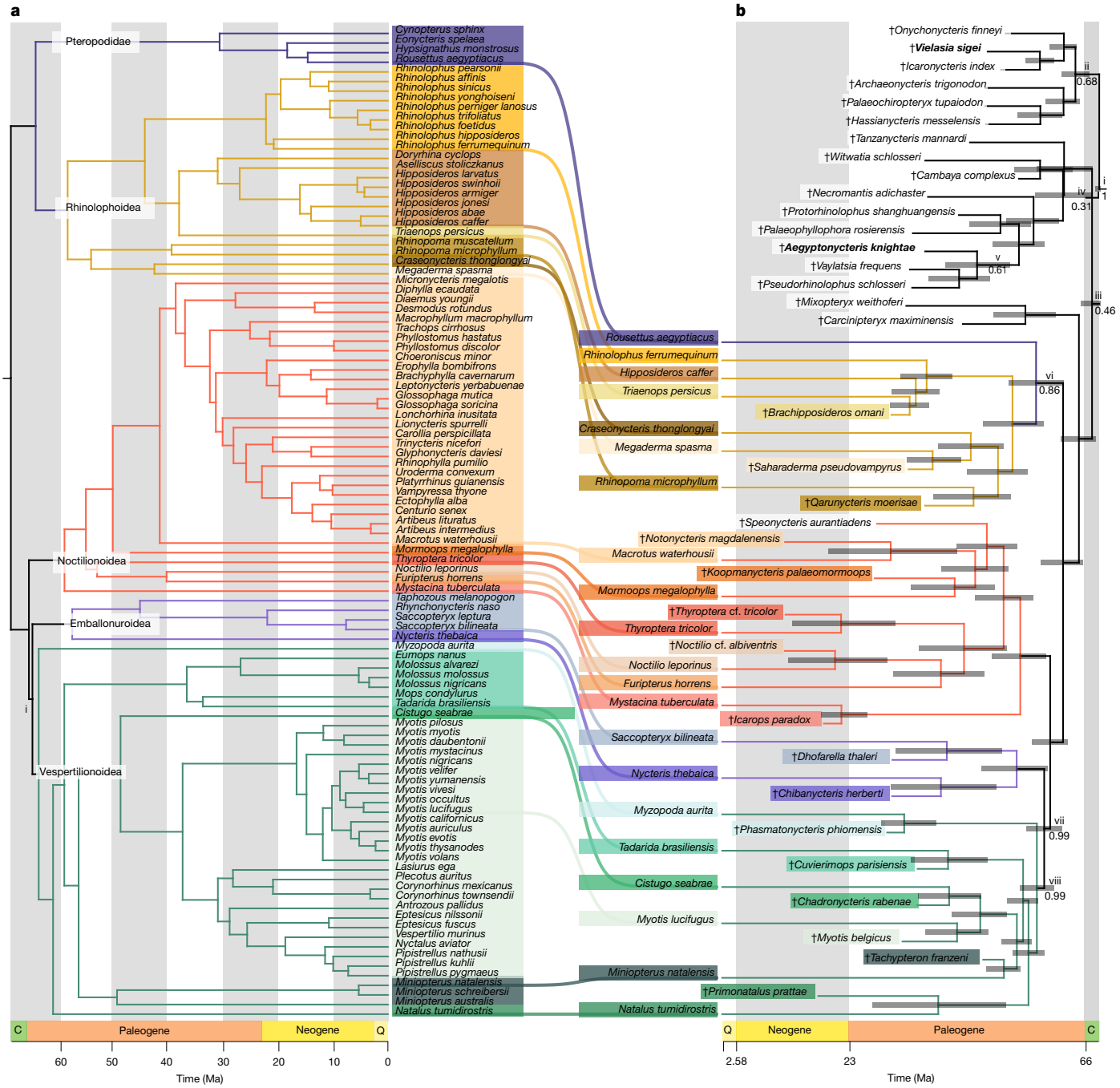

Fig. 2 | Timetrees based on node-based and tip-dating approaches with geological timescales. a, Mean divergence times from Bayesian analyses of coding sequences and fossil-based constraints on the T2 tree. The sister relationship between the superfamilies Emballonuroidea and Vespertilionoidea is also shown (i). C, Cretaceous; Q, Quaternary. **b**, Divergence times based on total evidence dating including fossils as tips under the fossilized birth–death process, or tip dating, with posterior probabilities of key node support: (i) Chiropteran root placement. (ii) Oldest branching bat clade, Eochiroptera, including the laryngeal echolocating species †*Vielasia* highlighted in bold. (iii) Unnamed clade comprising the sister to the redefined Eochiroptera. (iv) Unnamed clade comprising both laryngeal echolocating species and the oldest bat inferred to feed on plants, †*Aegyptonycteris*, highlighted in bold. (v) Unnamed and smallest clade. (vi) Yinpterochiroptera. (vii) The sister relationship between the superfamilies Emballonuroidea and Vespertilionoidea, and (viii) Vespertilionoidea including Myzopodidae.

and Supplementary Notes 9 and 10). However, only 22% of per-locus maximum-likelihood protein-coding gene trees supported this arrangement (M + V), with 16% supporting inclusion within Noctilionoidea (M + N) and 11% supporting a sister relationship with Emballonuroidea (M + E; Fig. 3b). No analyses supported an early branching position in Yangochiroptera. Using gene concordance factor (gCF) analyses, which quantifies gene tree concordance–discordance, we assessed the level of concordance per gene and found similar support for the alternate positions of Myzopodidae (gCF: 22.89% (M + V), 16.74% (M + N), 10.18% (M + E) and 50.19% (other); Supplementary Note 11). Only 22% of loci supported the position of Myzopodidae as sister to Vespertilionoidea (M + V). This placement received higher support than any alternative (Supplementary Table 11.1 and Supplementary Fig. 11.1). These results reveal extensive discordance among protein-coding genes, most likely driven by the alternate selection pressure on the functional proteins they encode and/or a lack of signal impeding the resolution of the true

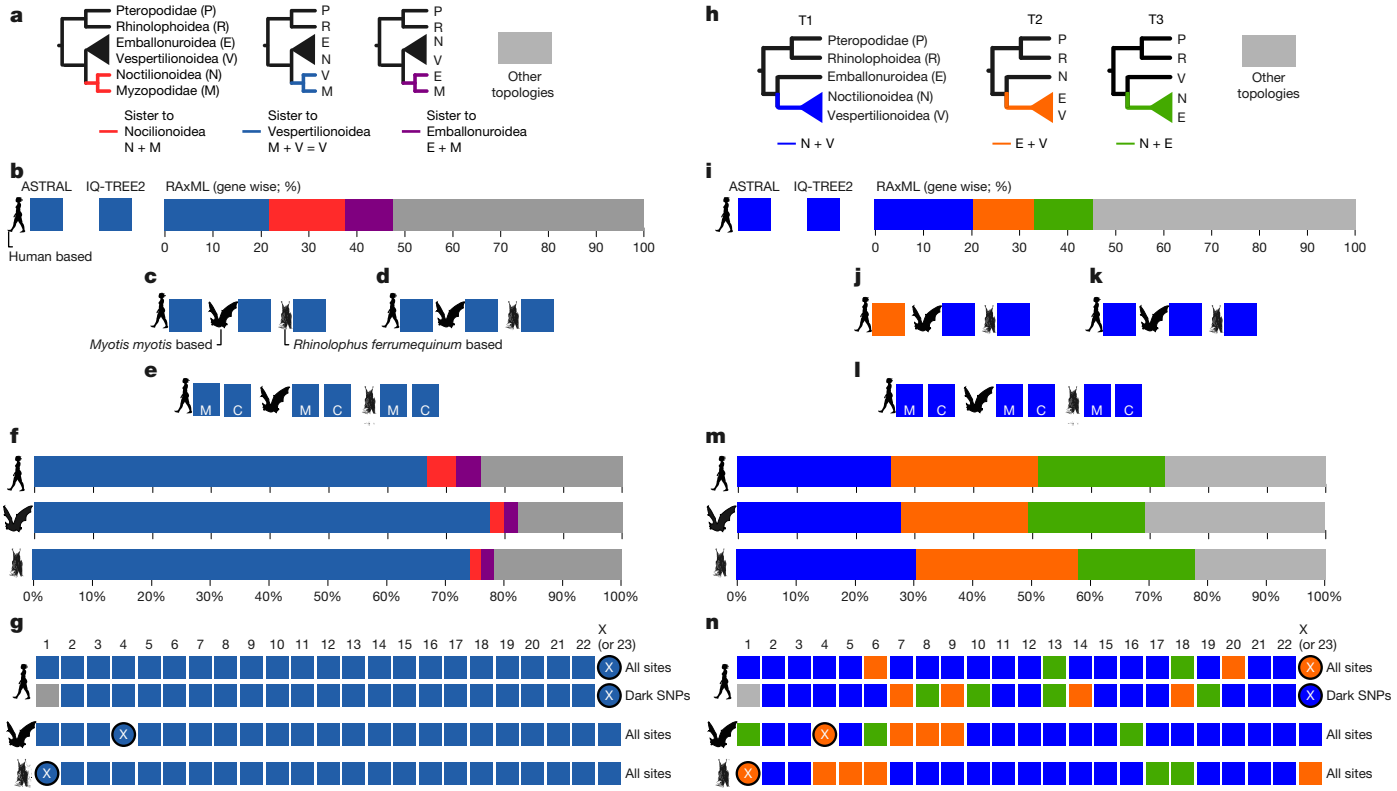

Fig. 3 | Genome-wide phylogenetic signal for the placement of Myzopodidae and relationships among yangochiropteran superfamilies. a, Alternative hypotheses tested for the phylogenetic position of Myzopodidae. **b**–**g**, Support for these hypotheses across distinct genomic data partitions. **h**, Alternative hypotheses for relationships among the three yangochiropteran superfamilies. Myzopodidae is considered a member of the superfamily Vespertilionoidea. **i**–**n**, Corresponding support across the same genomic partitions. In panels **b**,**i**, single-locus and species trees inferred from protein-coding genes under coalescent and concatenated frameworks. In panels **c**,**j**, CASTER analyses of neutral genomic windows (500 bp or more) derived from MULTIZ alignments projected to human (left), *Myotis* (middle) and *Rhinolophus* (right). In panels **d**,**k**, CASTER analyses of neutral dark SNPs extracted from unannotated regions for MULTIZ alignments projected to human (left), *Myotis* (middle) and *Rhinolophus* (right). In panels **e**,**l**, whole-genome species trees inferred from reference-based MULTIZ (M) and reference-free CACTUS (C) alignments, each projected to the three reference species. In panels **f**,**m**, sliding-window analyses across chromosomes or scaffolds; the bars indicate the proportion of windows supporting each topology for each reference. In panels **g**,**n**, chromosome-level and scaffold-level phylogenies; the squares indicate autosomes and the circles indicate X chromosomes. For human-based alignments, the second row represents dark SNPs. The silhouettes of *M. myotis* and *R. ferrumequinum* were vectorized by A.E.M. from illustrations by Fiona Reid. The silhouette of *H. sapiens* was created using PhyloPic (https://phylopic.org) under a Creative Commons licence CC0 1.0.

branching patterns, showing how previous bat phylogenies based on protein-coding genes[17] could have been misled[34,35].

As protein-coding genes comprise approximately 2% of the genome and can be vulnerable to model misspecification[6,34] and/or selection bias[34,36], we next analysed the whole-genome signal across multiple partitions and across our different whole-genome alignments. The partitions included neutral intergenic regions, neutrally evolving 'dark' SNPs (defined below; Supplementary Note 12), autosomes, the X chromosome and non-overlapping sliding windows with boundaries guided by genic features to avoid splitting genes (Supplementary Notes 9 and 12).

First, following evidence that neutrally evolving regions can minimize systematic biases resulting from selection[35], we used per-base phyloP scores and phastCons to exclude both site-wise accelerated or conserved positions and contiguous constrained regions, as well as genic regions, retaining windows 500 bp or more of neutral sequences (total for mHR, mMR and mRR ≈ 43, 48 and 78 Mb, respectively; Supplementary Note 9). Second, we analysed unconstrained and unannotated genomic regions, which we refer to as the 'dark genome', by excluding all known annotated regions from our alignments (Supplementary Note 12). We used our phyloP scores to identify and extract the neutral dark SNPs shared by all taxa from these regions (Supplementary Note 12). We further reduced systematic biases, by using CASTER, a phylogenomic method that relaxes the requirement for recombination-free loci and accounts for incomplete lineage sorting (ILS) and rate heterogeneity[34]. CASTER analyses of both neutral windows (mHR, mMR and mRR bootstrap = 100, 100 and 100%; q1 = 0.51, 0.48 and 0.50%, respectively; Fig. 3c and Supplementary Note 9) and neutral dark SNPs (mHR, mMR and mRR bootstrap = 99.7, 100 and 74.5%; q1 = 0.403, 0.631 and 0.356, respectively; Fig. 3d and Supplementary Note 12) unambiguously supported Myzopodidae as the earliest branch within Vespertilionoidea (M + V; Fig. 2a).

Given that neutral datasets represented only approximately 0.1–3% of genomes, we further tested the robustness of our topology by analysing whole-genome, whole-scaffold and whole-autosome datasets using CASTER (Supplementary Notes 9 and 12). All analyses predominantly supported Myzopodidae as sister to Vespertilionoidea (M + V; Fig. 3e–g and Supplementary Fig. 9.1a–d). In addition, gCF indicated a consistent signal across all datasets, with optimal topologies showing the strongest support for Myzopodidae as sister to Vespertilionoidea (Supplementary Table 11.1, Supplementary Fig. 11.2 and Supplementary Note 11).

In summary, across protein-coding genes, multiple genomic partitions and alignment frameworks, we consistently recovered a revised topology differing from prevailing molecular hypotheses in the placement of Myzopodidae (Fig. 2a). Of note, this topology agrees with the

total evidence molecular + morphology-based topology (Fig. 2b). These results warrant a revision of the biogeographical history of bats and the inclusion of Myzopodidae within the superfamily Vespertilionoidea.

Bat superfamily relationships

One branch that had variable support across datasets and analyses was the position of the superfamily Emballonuroidea within the suborder Yangochiroptera. This branch is notoriously short and challenging to resolve[13,17]. We used the same data partitioning and inference approaches (Supplementary Notes 9–12) to evaluate the competing hypotheses (Emballonuroidea (Vespertilionoidea + Noctilionoidea); T1); (Noctilionoidea (Vespertilionoidea + Emballonuroidea); T2); and (Vespertilionoidea (Emballonuroidea + Noctilionoidea); T3; Fig. 3h).

Across the protein-coding datasets, both coalescent and concatenated analyses recovered congruent highly supported topologies for T1 (Fig. 3i; coalescent and concatenated bootstrap = 100 and 100%, respectively). However, per-locus maximum-likelihood protein-coding gene trees (T1, T2, T3 and other = 21, 13, 12 and 54%) and gCF (T1, T2, T3 and other = 21, 13, 11 and 55%) showed discordant support per gene, highlighting the conflicting signal in the protein-coding genes, as was expected (Fig. 3i). Neutral-region analyses also revealed discordance across datasets (Fig. 3j,k). CASTER analyses of mHR neutral windows recovered (T2; bootstrap = 89.9%, q1 = 34), but neutral window analyses of both bat-reference MULTIZ alignments (mRM and mRR bootstrap = 100 and 99%; q1 = 35 and 34, respectively; Fig. 3j) and analyses of neutral dark SNPs (mHR, mRM and mRR bootstrap = 96.4, 100 and 100%; q1 = 0.383, 0.428 and 0.393, respectively; Fig. 3k) optimally supported T1 (Extended Data Fig. 9).

Whole-genome analyses, regardless of alignment reference species and methods, all supported T1 (Fig. 3l). However, analyses using dark SNPs from different evolutionary rate categories resulted in heterogeneous topological support (Extended Data Fig. 9), highlighting discordance across the genomes (Supplementary Note 12). Sliding-window analyses across MULTIZ alignments for all references, provided near similar support for all hypotheses (T1, T2 and T3; Fig. 3m and Supplementary Fig. 9.1). These results were mirrored by gCF, which indicated a slight overall excess of support for T2 (Supplementary Tables 11.1 and 11.2 and Supplementary Figs. 11.1 and 11.2). Chromosome-level and scaffold-level trees (Fig. 3n) further highlighted this topological heterogeneity (Supplementary Fig. 12.5). Although a slight majority of genomic regions across all references supported T1, the X chromosome in all three references along with a subset of autosomes consistently supported T2 (Fig. 3n and Supplementary Fig. 12.5).

Widespread phylogenetic incongruence among chromosomes indicates that pronounced phylogenomic discordance characterizes the evolutionary history of Yangochiroptera, with different genomic compartments (loci) supporting alternative topologies, particularly T1 and T2. Such heterogeneity in locus tree topology can arise from locus tree estimation errors, ILS and introgression. Although locus tree estimation artefacts cannot be entirely excluded, we consider their influence to be limited given the high concordance of results across multiple alignment and phylogenetic reconstruction strategies (Fig. 3). Likewise, although ILS can generate topological conflict among loci, under ILS alone, the species tree is expected to remain the predominant genomic signal across genomic compartments, including autosomes and the X chromosome[15,35,37,38]. Therefore, the extensive chromosome-scale discordance recovered here cannot be explained by ILS alone and is more consistent with the genomic compartmentalization expected under pervasive introgression[37] (Supplementary Note 13). Introgression is well known to produce such genomic heterogeneity by causing different genomic regions to retain distinct histories of lineage divergence and secondary gene exchange[39,40]. In clades experiencing pervasive introgression, phylogenetic analyses based on the whole genome may therefore recover the dominant history of introgressed ancestry (here T1) rather than the underlying species tree (T2)[39,40]. Under this framework, the true branching history of lineages is expected to persist primarily in low-recombining genomic regions, where the incorporation of foreign alleles is more strongly constrained by selection[15,41].

In mammals, the X chromosome, particularly the X-linked recombination desert region (XLRD), is characterized by exceptionally low recombination rates relative to the rest of the genome[38], making it less permeable to introgressed ancestry and therefore more likely to retain the underlying species-tree signal. CASTER topologies generated from this XLRD region supported T2 (Extended Data Figs. 5 and 10 and Supplementary Note 13). These results indicate that widespread genomic support for T1 reflects a dominant signal most likely generated by introgression; whereas T2 represents the underlying species tree. Topology (T2) is also congruent with the combined molecular and morphological analyses (Fig. 2b), further supporting a deep evolutionary separation between Noctilionoidea and the sister-assemblage Vespertilionoidea + Emballonuroidea.

The ancestral bat karyotype

Given that Chiroptera is the second-most speciose order of mammals[2], reconstructing its ancestral karyotype has been challenging. Zoo-fluorescent in situ hybridization (Zoo-FISH) data have suggested that the ancestral bat genome probably comprised 26 conserved chromosomal fragments; however, reconstructions of the ancestral chromosomes have not yet been achieved[42]. We reconstructed the ancestral bat karyotype and the syntenic relationships using LASTZ chain-and-net alignments for the 103 bat assemblies and the eight outgroups, aligned against two references representing Yangochiroptera (*M. myotis*) and Yinpterochiroptera (*R. ferrumequinum*). These alignments were analysed with DESCHRAMBLER[43,44] with a 300-kb syntenic fragment resolution (Supplementary Note 15).

We identified 30 reconstructed ancestral chromosome fragments (RACFs) covering 83.5% of the *R. ferrumequinum* genome and 32 RACFs covering 80.6% of the *M. myotis* genome. The direct and indirect comparison of RACFs between *R. ferrumequinum* and *M. myotis* reconstructions revealed a high consistency of RACF structures. There were only four interchromosomal and seven intrachromosomal differences across the entire genome, involving 1.4% of the ancestral genome sequence (Supplementary Figs. 15.1 and 15.2).

To investigate the reproducibility of our reconstructions, we generated two additional ancestral karyotypes using ingroup assemblies with high coverage of the corresponding references in syntenic fragments (Supplementary Tables 15.1–15.5 and Supplementary Note 15). The final reconstruction consisted of 26 ancestral bat chromosomes (Fig. 4), agreeing with the number of 'evolutionarily conserved units' predicted by Zoo-FISH[45].

Fusions of ancestral chromosomes prevail over fissions in 97% of the bat genomes (n = 100 of 103) and in 95% of the representative species (n = 20 of 21; Fig. 4). This suggests that bat karyotypes evolved through the fusion of ancestral chromosomes with fissions and translocations being less common. For example, ancestral bat chromosome 13 is found as an individual chromosome, or merged with other ancestral chromosomes in 18 of 21 representative species. Comparisons among human and bat chromosomes using Zoo-FISH revealed seven fusions of human chromosome syntenies ancestral to Chiroptera[42,46], of which five were found in our RACFs and two in the ancestral bat chromosomes. These fusions can be seen on the 'human' panel of Fig. 4. Our reconstruction also contained all seven mammalian ancestral human chromosome associations reported for the bat ancestor[42,46], all of which were found in RACFs, confirming the high integrity and accuracy of the reconstruction (Fig. 4 and Supplementary Table 15.7).

Cytogenetic studies have highlighted difficulties in resolving the ancestral bat karyotype due to extensive Robertsonian translocations,

Fig. 4 | Reconstructing the ancestral bat karyotype (1*n* = 26) and relationship between ancestral chromosome fragments in representative species of 21 bat families. The top panel shows the chiropteran ancestral chromosomes (lower part) painted with human chromosomes (upper part). The numbers under the panel represent 26 chiropteran ancestral chromosomes, with letter extensions denoting RACF order within a chromosome. The ancestral chromosomes are ordered by synteny with extant species scaffolds, not by numbers. The subsequent panels illustrate paintings of the longest scaffolds from representative genomes of 21 bat families, selected based on the highest coverage of the reference genome and a lower chromosome number within the family, featuring chiropteran ancestral chromosome colours. Species order numbers and families are shown to the left of the scaffolds: (1) *Lasiurus ega* (Vespertilionidae), (2) *Cistugo seabrae* (Cistugidae), (3) *Miniopterus natalesis* (Miniopteridae), (4) *Molossus alvarezi* (Molossidae), (5) *Natalus tumidirostris* (Natalidae), (6) *Myzopoda aurita* (Myzopodidae), (7) *Macrophyllum macrophyllum* (Phyllostomidae), (8) *Mormoops megalophylla* (Mormoopidae), (9) *Furipterus horrens* (Furipteridae), (10) *Noctilio leporinus* (Noctilionidae), (11) *Thyroptera tricolor* (Thyropteridae), (12) *Mystacina tuberculata* (Mystacinidae), (13) *Taphozous melanopogon* (Emballonuridae), (14) *Nycteris thebaica* (Nycteridae), (15) *Hipposideros armiger* (Hipposideridae), (16) *Triaenops persicus* (Rhinonycteridae), (17) *R. ferrumequinum* (Rhinolophidae), (18) *Craseonycteris thonglongyai* (Craseonycteridae), (19) *Megaderma spasma* (Megadermatidae), (20) *Rhinopoma muscatellum* (Rhinopomatidae) and (21) *Cynopterus sphinx* (Pteropodidae). The lines within the coloured blocks indicate the orientation of the synteny segments. The grey ribbon lines connect homologous synteny segments of the chiropteran ancestor across the bat family representatives. The black arrowheads above scaffolds indicate positions of the major ancestral chromosome fusions in extant species genomes. The numbers to the right of the scaffolds indicate the total number of ancestral chromosome fusions/fissions in the corresponding scaffold set. The colour codes on the right demarcate the chiropteran ancestor chromosomes (1–25 and X). The same colours were used for human chromosomes (1–22 and X).

including multiple recurrent rearrangements[42,47]. The small number of fragmented chromosomes suggests that recurrent rearrangements may have complicated ancestral chromosome reconstructions, despite using the highly contiguous assemblies and high-resolution alignments. Although our ancestral chromosome number matches the number of predicted ancestral bat evolutionary conserved units, we cannot exclude the possibility that some of our ancestral chromosomes represent chromosome arms. Many of the RACFs are identifiable as synteny blocks in extant bat karyotypes, which are known to evolve through the fusion of ancestral chromosomes, supporting this interpretation[42]. Alternatively, the X chromosome, which is known to be (sub) metacentric in many mammals, including bats[48,49], was assembled into one RACF, suggesting that our approach is capable of crossing at least some ancestral centromeres. A comparison of our reconstruction with the syntenies of human chromosomes inferred by Zoo-FISH[42] confirmed the presence of all predicted fusions reported for the bat ancestor.

Fossils, morphology and molecular dating

Resolving and dating the bat phylogeny has been central to understanding the origins of flight, echolocation and other key bat adaptations (Supplementary Note 16). However, determining how fossil bats relate to living families and when the lineages evolved required tackling major challenges: (1) the paucity of either fossils in morphological datasets[16], or of living taxa in dating analyses of combined morphological and molecular characters[50]; (2) bias in inferring phylogenies from saturated[51] and/or non-independent morphological characters[52]; and (3) using inappropriate evolutionary models that assume both character independence and linear character-state accumulation[53].

To overcome these obstacles, we first assembled a large morphological dataset of 44 pre-Quaternary fossil taxa comprising all but four of the living families and four clades of Eocene stem bats[16]. We also included a representative of every extant bat family, choosing species to match our genome assemblies (Supplementary Notes 16 and 17). The resulting data matrix (n = 699 characters), consisted of 65 species, 21 extant and 44 extinct, with 11 newly scored in this study. After filtering saturated and non-independent morphological characters[54] (Supplementary Table 16.2), we identified 480 statistically independent characters and retained a single fossil per family with the most characters scored. We next subsampled a dataset of 10,000 neutrally evolving sites from intergenic neutral windows in the mHR alignment per species, and merged this with our filtered morphological dataset

(Supplementary Note 9). We analysed this total evidence dataset by adopting a fossilized birth–death or total evidence dating (TED)[55] approach that simultaneously models fossilization, taxon sampling and birth–death branching processes[56] to estimate divergence dates, thus overcoming challenges that hindered past studies.

Previous analyses identified the oldest stem bats by designating outgroups[16], or enforcing bat monophyly to determine the placement of the newly described Eocene taxon: †*Vielasia*[50]. By contrast, our TED approach directly inferred the root by identifying the oldest branch: a clade containing the extinct families Archaeonycteridae, Onychonycteridae, Icaronycteridae, Hassianycteridae, Palaeochiropterygidae and †*Vielasia* (Fig. 2b, clade i, 100% posterior probability as a percentage (pp); see Supplementary Fig. 17.2). Previously thought to represent an early diverging paraphyletic grade of stem bats instead of a clade[57], these families (minus †*Vielasia*) have nonetheless been referred to as 'Eochiroptera' (sensu Van Valen[58]). Including †*Vielasia* in this new Eochiroptera with medium probability (Fig. 2b, clade ii, 68% pp) bolsters support for the finding by Hand et al.[50] that the evolution of laryngeal echolocation predates the crown-bat radiation.

We found a second clade of stem Eocene bats that resembles modern Yinpterochiroptera, by including lineages inferred as capable of laryngeal echolocation and the first instance of bat herbivory (Fig. 2b, clade iv, 31% pp). †*Palaeophyllophora*, †*Protorhinolophus*, †*Pseudorhinolophus* and †*Vaylatsia* were previously thought to belong in Rhinolophoidea, but Jones et al.[16] has found them among the earliest diverging clade of bats together with representatives of the extinct family Necromantidae, †*Necromantis adichaster* and †*Cambaya complexus*. In common with previous morphological analyses[16], we found a clade comprising the echolocating lineages formerly classified as 'Rhinolophoidea,' †*Necromantis* and †*Cambaya*, but our result also includes a representative of the family Philisidae (†*Witwatia schlosseri*). Although support for this clade is weak (31% pp), support for †*Aegyptonycteris*, the earliest example of bat omnivory[59], nesting within the former stem 'Rhinolophoidea', is moderate (Fig. 2b, clade v, 61% pp). Echolocation use by †*Aegyptonycteris* is unknown, but our results indicate the ancient, independent evolution of omnivorous or herbivorous taxa from echolocating, presumed insectivorous ancestors. Together with extant instances in Yinpterochiroptera and Phyllostomidae, this result suggests high evolvability for sensory and dietary adaptations in bats.

Past total evidence and morphology-based inferences among living bat lineages are consistent with most genomic analyses, with one exception, the suborder Yinpterochiroptera, supporting instead the monophyly of the echolocating lineages in the traditional suborder Microchiroptera[16,50]. We found strong support for yinpterochiropteran monophyly (Fig. 2b, clade vi, 86% pp), indicating concordance in phylogenetic signal for this clade using combined morphological + molecular data and a fossilized birth death model, without having to constrain the monophyly of Yinpterochiroptera as previously required[16].

How the poor fossil record of bats[17,19] impacts dating analyses is hard to discern[60]. In the first analysis of its kind, an average 73% of molecular branch length was estimated missing from the fossil record constituting unrepresented basal branch lengths (UBBLs)[17]. However, such node-based dating analyses tend to overestimate divergence times compared with fossil evidence[61]. Our TED approach significantly reduced ghost lineages and thus UBBLs across the bat phylogeny. With updated taxonomic sampling and filtered morphological characters, we found a mean of 48.7% (45.5% upper fossil boundary) from the TED tree, and 50.8% (47.8% lower fossil boundary) branch length missing from each family lineage in the genomic phylogeny (Supplementary Tables 17.2 and 17.5). Although subtle when averaged, UBBL reduction is significant across families ($P \leq 0.005$; Supplementary Note 17). Compared with both past and current molecular phylogenies, our TED results reconcile relaxed clock divergences with the limited yet growing bat fossil record.

By leveraging the age of all 44 fossils, results from combined data analyses also track bat macroevolutionary dynamics. Unlike past studies[21,62], we modelled both speciation and extinction rates directly while inferring the phylogeny and including fossil species that enable more robust estimates of extinction rates[63]. With a mean of 0.314 species per Ma, our speciation rate triples previously published[21,62] single-rate estimates. Similarly, our estimated extinction rate of 0.270 species per Ma was nine-times higher than previous studies[21], yielding a turnover of 0.844 species per Ma (see Supplementary Table 17.4). These results reveal systematic underestimates of both speciation rates and evolutionary turnover in the global bat radiation in previous analyses.

Biogeography

Where bats originated still remains an open question[17,20–22]. The poor fossil record[19,64] and the fact that all bats fly have hindered its resolution. Flight confers extraordinary dispersal capabilities and results in global distributions, thus obscuring biogeographical signal. Thus, we implemented a dispersal–extinction cladogenesis model with time-dependent, distance-informed dispersal penalties, accounting for continental drift and high bat mobility. We revisited this question by integrating our fossil and extant taxa into a biogeographical framework (Supplementary Note 18).

Previous fossil-informed analyses placed the origin of bats in North America[17], whereas early biogeographical models pointed to Africa[20], and more recent time-stratified approaches based on extant taxa alone, inferred Asia[21]. Our results instead reveal a late Paleocene ancestor (Fig. 2b, clade i, and Fig. 5a) that originated in Europe (99.2% pp), and whose descendants dispersed most probably to Africa (Figs. 2b, clade iii, and 5a and Supplementary Table 18.5). From this central Europe–Africa hub, we inferred multiple, independent range expansions into the Americas, Asia and Australia as modern bats diversified into their four major superfamilies (Fig. 25) within a narrow time interval in the early Eocene (Fig. 5b). For example, Yinpterochiroptera originated in Africa 57.1 Ma (Figs. 2b, clade v, 5c; Africa: 55.6% pp, Europe–Africa: 14.5% pp), expanding into Asia by the middle of the Eocene at the most recent common ancestor (MRCA) of the Hipposideridae, Rhinonycteridae, Rhinolophidae families (Fig. 5c; 26.3% pp for Asia and 31.1% for Asia–Africa).

Despite difficulties resolving the ancestral range of Yangochiroptera, probably because of rapid lineage emergence just after the Paleocene–Eocene thermal maximum (Supplementary Note 18), distinct patterns emerge from many of its constituent superfamilies. For example, the MRCA of Emballonuroidea and Vespertilionoidea resided in Europe and Africa (39.2% pp for Europe, 22.0% pp for Europe–Africa and 18.5% pp for Africa). The MRCA of Emballonuroidea came out of Africa (47.1% pp for Africa and 14.4% for Africa–Europe), whereas Vespertilionoidea, including Myzopodidae, diversified from a European ancestor (46.3% pp for Europe and 24.7% pp for Europe–Africa), with multiple subsequent colonizations of North America by Natalidae, Molossidae and the MRCA of Cistugidae and Vespertilionidae (Fig. 5c).

In the superfamily Noctilionoidea, we inferred a major dispersal from Europe (38.9% pp) into North America (47.2% pp) around 54 Ma (Fig. 5c). Both timing and topology of this scenario favour a North Atlantic landmass route during peak faunal exchange between Europe and North America during the late Eocene[65], instead of a Beringian pathway[21] (Fig. 5b). Following this initial expansion, we found strong support for a colonization of South America by the noctilionoids (52.3% pp) between 51 and 44 Ma (Fig. 5c). Our model rejects dispersal between Africa and South America (0.27% pp) by island hopping across the Atlantic[20]. Instead, the timing and route of noctilionoids reaching the Americas coincides with the expansion of the tropics in the middle latitudes of the Americas and Europe[66] and the beginning of the uplift of islands of the Panama isthmus[67], providing habitat and a North American route for this radiation of bats.

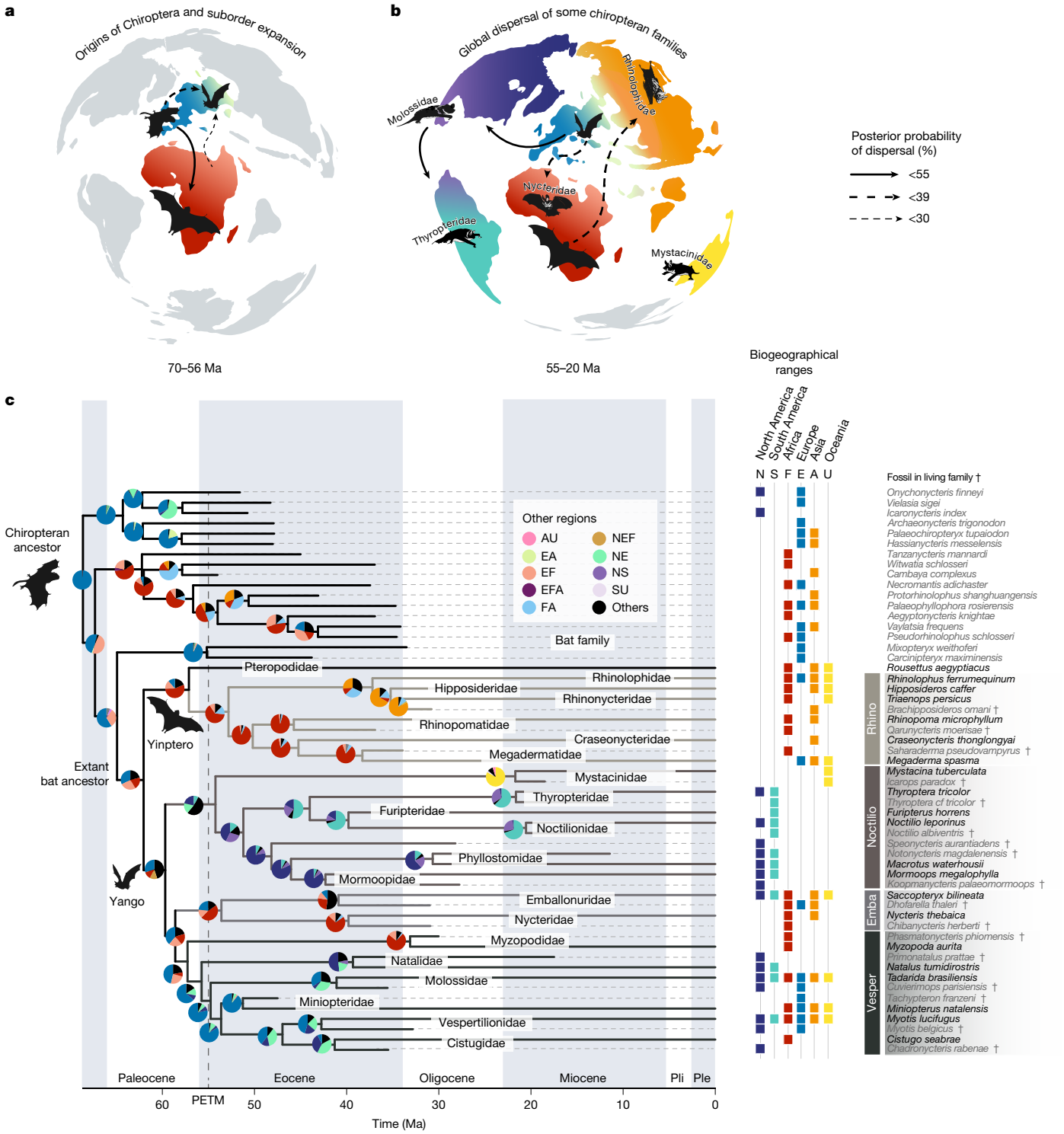

Fig. 5 | Paleogeographical origins and worldwide expansion of Chiroptera: Palaeocene–Eocene dispersal of bats from their area of origin. **a**, Geographical origins of Chiroptera and the suborders Yinpterochiroptera and Yangochiroptera. **b**, Eocene-to-Oligocene dispersal of bat families. **c**, Fossilized birth death tree, with dispersal–extinction cladogenesis biogeographical range posterior probabilities shown as pie charts at the nodes. Superfamilies included: Rhinolophoidea (Rhino), Noctilionoidea (Noctilio), Emballunoroidea (Emba) and Vespertilionoidea (Vesper). AU, ZZZ; EA, ZZZ; EF, ZZZ; EFA, ZZZ; FA, ZZZ; NE, ZZZ; NEF, ZZZ; NS, ZZZ; PETM, Palaeocene–Eocene thermal maximum; SU, ZZZ. The chiropteran ancestor silhouette was vectorized by F.X.C. from an *Onychonycteris* illustration on Dinopedia (https://dinopedia.fandom.com) under a Creative Commons licence CC-BY-SA. The 'Yinptero' silhouette was vectorized by F.X.C. from an illustration of an unidentified species of the family Pteropodidae on Crezilla (https://creazilla.com) by Natasha Sinegina under a Creative Commons licence CC BY 4.0. The 'Yango' silhouette was vectorized by A.E.M. from an illustration of *M. myotis* under a Creative Commons licence CC-BY-SA. Silhouettes of Molossidae (*Tadarida brasiliensis*), Thyropteridae (*Thyroptera tricolor*), Nycteridae (*Nycteris hispida*), Mystacinidae (*Mystacina tuberculata*) and Rhinolophidae (*Rhinolophus megaphyllus*) were vectorized by F.X.C. from illustrations by Fiona Reid. Data for the continent illustrations were from PaleoMAP (https://chronosphere.info/data/paleomap/) under a Creative Commons licence CC BY 4.0.

Conclusion

We overcame challenges that have hindered our understanding of bat evolutionary history, by integrating reference-quality whole-genome assemblies from all living bat families with a comprehensive morphological dataset including extant and extinct bats. We used innovative phylogenomic analyses accounting for complex evolutionary histories of both lineages and markers and generated a new phylogeny, resolving previous uncertainties at the superfamily level and placing the family Myzopodidae within Vespertilionoidea. We showed that bats, and thus powered flight, most likely originated in Europe in the late Palaeocene, refuting previous African and North American origins, and suggest that the acquisition of laryngeal echolocation predates the diversification of crown group bats, given the placement of the fossil †*Vielasia* in the oldest Eochiroptera clade. This suggests a close connection between flight and echolocation in the evolution of the ancestral bat lineage. Our analyses showed that Yinpteropchiroptera originated in Africa in the early Eocene with later dispersal of modern yinpterochiropteran families into Asia and Europe, with Yangochiroptera most likely originating in Europe within a similar timeframe. The bat superfamilies probably radiated during the Paleocene–Eocene thermal maximum (approximately 56 Ma) coinciding with increased global temperature and environmental change. Chromosomal reconstructions supported 26 ancestral bat chromosomes and showed that modern bat genomes most likely evolved through chromosome fusions instead of fissions or translocations, shedding light on evolutionary constraints pertaining to the smallest mammalian genomes. The multiple genome alignments and datasets represent valuable resources for the genomics community. Given that they are based on the same set of genome assemblies, they enable benchmarking and direct methodological comparisons among alignment approaches. Finally, the methodological framework presented here can be applied to address phylogenomic questions in other taxonomic groups.

Online content

Any methods, additional references, Nature Portfolio reporting summaries, source data, extended data, supplementary information, acknowledgements, peer review information; details of author contributions and competing interests; and statements of data and code availability are available at https://doi.org/10.1038/s41586-026-11007-3.

1. Teeling, E. C. et al. Bat biology, genomes, and the Bat1K project: to generate chromosome-level genomes for all living bat species. *Annu. Rev. Anim. Biosci.* **6**, 23–46 (2018).
2. Simmons, N. B. & Cirranello, A. L. Bat species of the world: a taxonomic and geographic database v1.9. *Bats of the World* https://www.batnames.org/species/about.html (2025).
3. Cooper, L. N. et al. Bats as instructive animal models for studying longevity and aging. *Ann. N. Y. Acad. Sci.* **1541**, 10–23 (2024).
4. Déjosez, M. et al. Bat pluripotent stem cells reveal unusual entanglement between host and viruses. *Cell* **186**, 957–974.e28 (2023).
5. Morales, A. E. et al. Bat genomes illuminate adaptations to viral tolerance and disease resistance. *Nature* **638**, 449–458 (2025).
6. Jebb, D. et al. Six reference-quality genomes reveal evolution of bat adaptations. *Nature* **583**, 578–584 (2020).
7. Osmanski, A. B. et al. Insights into mammalian TE diversity through the curation of 248 genome assemblies. *Science* **380**, eabn1430 (2023).
8. Teeling, E. C., Dool, S. & Springer, M. S. Phylogenies, fossils and functional genes: the evolution of echolocation in bats. In *Evolutionary History of Bats* (eds Gunnell, G. F. & Simmons, N. B.) 1–22 (Cambridge Univ. Press, 2012).
9. Sulser, R. B., Patterson, B. D., Urban, D. J., Neander, A. I. & Luo, Z.-X. Evolution of inner ear neuroanatomy of bats and implications for echolocation. *Nature* **602**, 449–454 (2022).
10. Anderson, S. C. & Ruxton, G. D. The evolution of flight in bats: a novel hypothesis. *Mamm. Rev.* **50**, 426–439 (2020).
11. Springer, M. S., Teeling, E. C., Madsen, O., Stanhope, M. J. & de Jong, W. W. Integrated fossil and molecular data reconstruct bat echolocation. *Proc. Natl Acad. Sci. USA* **98**, 6241–6246 (2001).
12. Li, G., Wang, J., Rossiter, S. J., Jones, G. & Zhang, S. Accelerated FoxP2 evolution in echolocating bats. *PLoS ONE* **2**, e900 (2007).
13. Hao, X., Lu, Q. & Zhao, H. A molecular phylogeny for all 21 families within Chiroptera (bats). *Integr. Zool.* **19**, 989–998 (2024).
14. Wang, L.-F., Gamage, A. M., Chan, W. O. Y., Hiller, M. & Teeling, E. C. Decoding bat immunity: the need for a coordinated research approach. *Nat. Rev. Immunol.* **21**, 269–271 (2021).
15. Foley, N. M. et al. Karyotypic stasis and swarming influenced the evolution of viral tolerance in a species-rich bat radiation. *Cell Genom.* **4**, 100482 (2024).
16. Jones, M. F., Beard, K. C. & Simmons, N. B. Phylogeny and systematics of early Paleogene bats. *J. Mammal Evol.* https://doi.org/10.1007/s10914-024-09705-8 (2024).
17. Teeling, E. C. et al. A molecular phylogeny for bats illuminates biogeography and the fossil record. *Science* **307**, 580–584 (2005).
18. Brown, E. E., Cashmore, D. D., Simmons, N. B. & Butler, R. J. Data from: quantifying the completeness of the bat fossil record. *Dryad* https://doi.org/10.5061/DRYAD.HP250FB (2019).
19. Eiting, T. P. & Gunnell, G. F. Global completeness of the bat fossil record. *J. Mamm. Evol.* **16**, 151–173 (2009).
20. Eick, G. N., Jacobs, D. S. & Matthee, C. A. A nuclear DNA phylogenetic perspective on the evolution of echolocation and historical biogeography of extant bats (Chiroptera). *Mol. Biol. Evol.* **22**, 1869–1886 (2005).
21. Yu, W., Wu, Y. & Yang, G. Early diversification trend and Asian origin for extent bat lineages. *J. Evol. Biol.* **27**, 2204–2218 (2014).
22. Springer, M. S., Meredith, R. W., Janecka, J. E. & Murphy, W. J. The historical biogeography of Mammalia. *Phil. Trans. R. Soc. B* **366**, 2478–2502 (2011).
23. Blaxter, M. et al. The Earth BioGenome Project Phase II: illuminating the eukaryotic tree of life. *Front. Sci.* **3**, 1514835 (2025).
24. Hubley, R. et al. The Dfam database of repetitive DNA families. *Nucleic Acids Res.* **44**, D81–D89 (2016).
25. Paulat, N. S. et al. Chiropterans are a hotspot for horizontal transfer of DNA transposons in mammalia. *Mol. Biol. Evol.* **40**, msad092 (2023).
26. Paulat, N. S. et al. Transposable elements in bats show differential accumulation patterns determined by class and functionality. *Life* **12**, 1190 (2022).
27. Cantrell, M. A., Scott, L., Brown, C. J., Martinez, A. R. & Wichman, H. A. Loss of LINE-1 activity in the megabats. *Genetics* **178**, 393–404 (2008).
28. Umu, S. U. et al. Accurate microRNA annotation of animal genomes using trained covariance models of curated microRNA complements in MirMachine. *Cell Genom.* **3**, 100348 (2023).
29. Blanchette, M. et al. Aligning multiple genomic sequences with the threaded blockset aligner. *Genome Res.* **14**, 708–715 (2004).
30. Armstrong, J. et al. Progressive Cactus is a multiple-genome aligner for the thousand-genome era. *Nature* **587**, 246–251 (2020).
31. Sharma, V. & Hiller, M. Increased alignment sensitivity improves the usage of genome alignments for comparative gene annotation. *Nucleic Acids Res.* **45**, 8369–8377 (2017).
32. Osipova, E., Hecker, N. & Hiller, M. RepeatFiller newly identifies megabases of aligning repetitive sequences and improves annotations of conserved non-exonic elements. *Gigascience* **8**, giz132 (2019).
33. Kirilenko, B. M. et al. Integrating gene annotation with orthology inference at scale. *Science* **380**, eabn3107 (2023).
34. Zhang, C., Nielsen, R. & Mirarab, S. CASTER: direct species tree inference from whole-genome alignments. *Science* **387**, eadk9688 (2025).
35. Foley, N. M. et al. A genomic timescale for placental mammal evolution. *Science* **380**, eabl8189 (2023).
36. Stiller, J. et al. Complexity of avian evolution revealed by family-level genomes. *Nature* **629**, 851–860 (2024).
37. Hibbins, M. S. & Hahn, M. W. Phylogenomic approaches to detecting and characterizing introgression. *Genetics* **220**, iyab173 (2022).
38. Foley, N. M. et al. An ancient recombination desert is a speciation supergene in placental mammals. *Nature* **649**, 1228–1236 (2026).
39. Burbrink, F. T., DeBaun, D., Foley, N. M. & Murphy, W. J. Recombination-aware phylogenomics. *Trends Ecol. Evol.* **40**, 900–912 (2025).
40. Mirarab, S. et al. A region of suppressed recombination misleads neoavian phylogenomics. *Proc. Natl Acad. Sci. USA* **121**, e2319506121 (2024).
41. Veller, C., Edelman, N. B., Muralidhar, P. & Nowak, M. A. Recombination and selection against introgressed DNA. *Evolution* **77**, 1131–1144 (2023).
42. Volleth, M. & Eick, G. Chromosome evolution in bats as revealed by FISH: the ongoing search for the ancestral chiropteran karyotype. *Cytogenet. Genome Res.* **137**, 165–173 (2012).
43. Kim, J. et al. Reconstruction and evolutionary history of eutherian chromosomes. *Proc. Natl Acad. Sci. USA* **114**, E5379–E5388 (2017).
44. Damas, J. et al. Evolution of the ancestral mammalian karyotype and syntenic regions. *Proc. Natl Acad. Sci. USA* **119**, e2209139119 (2022).
45. Volleth, M., Heller, K. G., Pfeiffer, R. A. & Hameister, H. A comparative ZOO-FISH analysis in bats elucidates the phylogenetic relationships between Megachiroptera and five microchiropteran families. *Chromosome Res.* **10**, 477–497 (2002).
46. Volleth, M., Yang, F. & Müller, S. High-resolution chromosome painting reveals the first genetic signature for the chiropteran suborder Pteropodiformes (Mammalia: Chiroptera). *Chromosome Res.* **19**, 507–519 (2011).
47. Benathar, T. C. M. et al. Karyotype, evolution and phylogenetic reconstruction in Micronycterinae bats with implications for the ancestral karyotype of Phyllostomidae. *BMC Evol. Biol.* **19**, 98 (2019).
48. Rodrigues, L. R. R. et al. Comparative cytogenetics of two phyllostomids bats. A new hypothesis to the origin of the rearranged X chromosome from *Artibeus lituratus* (Chiroptera, Phyllostomidae). *Caryologia* **56**, 413–419 (2003).
49. Fedyk, S. & Ruprecht, A. L. Chromosomes of some species of vespertilionid bats. II. Evolutionary relationships of plecotine bats. *Acta Theriol.* **28**, 8–9 (1983).
50. Hand, S. J., Maugoust, J., Beck, R. M. D. & Orliac, M. J. A 50-million-year-old, three-dimensionally preserved bat skull supports an early origin for modern echolocation. *Curr. Biol.* **33**, 4624–4640.e21 (2023).
51. Wagner, P. J. Exhaustion of morphologic character states among fossil taxa. *Evolution* **54**, 365–386 (2000).
52. Dávalos, L. M., Velazco, P. M., Warsi, O. M., Smits, P. & Simmons, N. B. Integrating incomplete fossils by isolating conflictive signal in saturated and non-independent morphological characters. *Syst. Biol.* **63**, 582–600 (2014).

53. Ronquist, F. et al. MrBayes 3.2: efficient Bayesian phylogenetic inference and model choice across a large model space. *Syst. Biol.* **61**, 539–542 (2012).
54. Herrera, J. P. & Dávalos, L. M. Phylogeny and divergence times of lemurs inferred with recent and ancient fossils in the tree. *Syst. Biol.* **65**, 772–791 (2016).
55. Heath, T. A., Huelsenbeck, J. P. & Stadler, T. The fossilized birth-death process for coherent calibration of divergence-time estimates. *Proc. Natl Acad. Sci. USA* **111**, E2957–E2966 (2014).
56. Zhang, C., Stadler, T., Klopfstein, S., Heath, T. A. & Ronquist, F. Total-evidence dating under the fossilized birth-death process. *Syst. Biol.* **65**, 228–249 (2016).
57. Simmons, N. B. & Geisler, J. H. *Phylogenetic Relationships of Icaronycteris, Archaeonycteris, Hassianycteris, and Palaeochiropteryx to Extant Bat Lineages* (American Museum of Natural History, 1998).
58. Van Valen, L. The evolution of bats. *Evol. Theory* **4**, 103–121 (1979).
59. Simmons, N. B., Seiffert, E. R. & Gunnell, G. F. A new family of large omnivorous bats (mammalia, Chiroptera) from the late Eocene of the fayum depression, Egypt, with comments on use of the name 'eochiroptera'. *Am. Mus. Novit.* **3857**, 1–43 (2016).
60. Ronquist, F., Lartillot, N. & Phillips, M. J. Closing the gap between rocks and clocks using total-evidence dating. *Phil. Trans. R. Soc. B* **371**, 20150136 (2016).
61. Wible, J. R., Rougier, G. W., Novacek, M. J. & Asher, R. J. Cretaceous eutherians and Laurasian origin for placental mammals near the K/T boundary. *Nature* **447**, 1003–1006 (2007).
62. Shi, J. J. & Rabosky, D. L. Speciation dynamics during the global radiation of extant bats. *Evolution* **69**, 1528–1545 (2015).
63. Silvestro, D., Warnock, R. C. M., Gavryushkina, A. & Stadler, T. Closing the gap between palaeontological and neontological speciation and extinction rate estimates. *Nat. Commun.* **9**, 5237 (2018).
64. Brown, E. E., Cashmore, D. D., Simmons, N. B. & Butler, R. J. Quantifying the completeness of the bat fossil record. *Palaeontology* **62**, 757–776 (2019).
65. Janis, C. M. Tertiary mammal evolution in the context of changing climates, vegetation, and tectonic events. *Annu. Rev. Ecol. Syst.* **24**, 467–500 (1993).
66. Morley, R. J. Cretaceous and tertiary climate change and the past distribution of megathermal rainforests. In *Tropical Rainforest Responses to Climatic Change* (eds Bush, M., Flenley, J. & Gosling, W.) 1–34 https://doi.org/10.1007/978-3-642-05383-2 (Springer Berlin Heidelberg, 2011).
67. Scotese, C. R., Song, H., Mills, B. J. W. & van der Meer, D. G. Phanerozoic paleotemperatures: the Earth's changing climate during the last 540 million years. *Earth Sci. Rev.* **215**, 103503 (2021).

Ariadna E. Morales[1,2,111], Yan Liang (梁妍)[3,112], William R. Thomas[4,112], Evgeny V. Leushkin[1,112], Francisco X. Castellanos[5,6,112], Denis M. Larkin[7,112], Tom Brown[8,112], Bastian Fromm[9,113], Suzanne J. Hand[10,113], Zixia Huang[11,113], Graham M. Hughes[11,12,113], Matthew F. Jones[13,113], Burton K. Lim[14,113], Meike Mai[15,113], Eugene W. Myers[3,8,16,113], Martin Pippel[8,17,18,113], Sebastien J. Puechmaille[2,19,113], Nancy B. Simmons[20,113], Linelle Ann L. Abueg[21], Nadav Ahituv[22,23], Zahran A. AlAbdulsalam[24], Ine Alvarez van Tussenbroek[15], Dineilys V. Aparicio[25], Lina M. Arcila Hernández[26,27], Alexander Ben Hamadou[1], Petr Benda[28,29], Mark Blaxter[3], Alex V. Borisenko[30,31], Jorge Brocca[32], Nair Cabezón[25], Lucia Carbone[33,34,35], Jose I. Carvajal[36], Wharton O. Y. Chan[37], Paul Davis[3], Dina K. N. Dechmann[25,38,39], Annette Denzinger[40], Judith L. Eger[14], Seth J. Eiseb[41,42], David Enard[43], Mark D. Engstrom[14,27], Nicole M. Foley[44,45], Giulio Formenti[21], Jackson Fuller[46], Ismael Galván[47], Akshamal M. Gamage[37], Neil J. Gemmell[48], Joanne E. Gillum[48], Alejandro Gonzales-Irribarren[1], Mailyn A. Gonzalez[49], Steven M. Goodman[50,51], Jonathan Gray[52], Carola Greve[1], Michael W. Guernsey[22,23,53], Edgar G. Gutiérrez[54], Yelena Guttman[22,23], Michael Hackenberg[55,56], Elena Hilario[36], Leon Hilgers[1,57], Thomas W. Horsley[14], Melissa R. de Waal[20,58], Deirdre M. Jafferally[59], Erich D. Jarvis[21,60], Sahieda A. Joemratie[61], Mirjam Knörnschild[25,62,63], Jenna E. Kohles[25,38,39], Dimitrios-Georgios Kontopoulos[1,64], Bonhwang Koo[21], M. Elise Lauterbur[43,65], Michael Letko[66], Harris A. Lewin[67], Shenglin Liu[1,57,68,69], Darrell K. Lizamore[70], Brian D. Lloyd[71], Livia Loureiro[72], M. Cristina MacSwiney G[73], Yury V. Malovichko[1,57], Kirsty McCaffrey[21], Dominik W. Melville[74], Magdalena Meyer[74], William O. Mgoola[46], Matthieu Muffato[3], Vincent J. Munster[75], William J. Murphy[44,45], Martina Nagy[63], Nicolas Nesi[76], Kimberly A. Nevonen[33], Haris Nicolaou[77], Evans E. Nkrumah[78], Norman Zacharias[79], Brian P. O'Toole[21], Sarah H. Olson[80], Alain Ondzie[81], Bismark A. Opoku[74], Jorge Ortega[54], William S. Pearman[48,82], Francy J. Perez-Llanos[83,84], Kendra L. Phelps[85], Myrtani Pieri[86], Sarahjane Power[11], Maksym Prylutskyi[7], Paola Pulido-Santacruz[87], Guoying Qi[3], Bernal Rodríguez-Herrera[88], Danny Rojas[89], Indranee Roopsind[90,91], Stephen J. Rossiter[92], Constance Scharff[93], Tilman Schell[1], Stephanie N. Seifert[66], Fernando Simal[94,95], Pipat Soisook[96], Simone Sommer[74], Andrew Spalton[97], Emma L. Stone[98,99], Peter H. Sudmant[100], Sam Talbot[21], Robert M. Timm[101,102], Laura Uelze[8,18], Nathan S. Upham[13], Marek Uvizl[11,28,29], Peter Vallo[103], Juan M. Vazquez[104], Lin-Fa Wang[37], Linet C. Watson[105], Daniel Whitby[106], Sylke Winkler[8,18], York Winter[62], Laurel R. Yohe[107], Monika Zavodna[108], Ning Zhang[52], Huabin Zhao[109], David A. Ray[5] ✉, Sonja C. Vernes[15] ✉, Liliana M. Dávalos[4,110] ✉, Michael Hiller[1,57] ✉ & Emma C. Teeling[3,11] ✉

[1]Senckenberg-Leibniz Institution for Biodiversity and Earth System Research, Senckenberganlage, Frankfurt, Germany. [2]University of Montpellier–CNRS–IRD, ISEM, Montpellier, France. [3]Tree of Life, Wellcome Sanger Institute, Hinxton, Cambridge, UK. [4]Department of Ecology and Evolution, Stony Brook University, New York, NY, USA. [5]Department of Biological Sciences, Texas Tech University, Lubbock, TX, USA. [6]Instituto Nacional de Biodiversidad, Quito, Ecuador. [7]Department of Comparative Biomedical Sciences, Royal Veterinary College, University of London, London, UK. [8]Max Planck Institute of Molecular Cell Biology and Genetics, Dresden, Germany. [9]The Arctic University Museum of Norway, UiT-The Arctic University of Norway, Tromso, Norway. [10]School of Biological, Earth and Environmental Sciences, UNSW Sydney, Sydney, New South Wales, Australia. [11]School of Biology and Environmental Science, University College Dublin, Dublin, Ireland. [12]Conway Institute, University College Dublin, Dublin, Ireland. [13]School of Life Sciences, Arizona State University, Tempe, AZ, USA. [14]Department of Natural History, Royal Ontario Museum, Toronto, Ontario, Canada. [15]School of Biology, University of St Andrews, St Andrews, UK. [16]Institute of Science and Technology, Okinawa, Japan. [17]SciLifeLab, National Bioinformatics Infrastructure Sweden (NBIS), Department of Cell and Molecular Biology, Uppsala University, Uppsala, Sweden. [18]DRESDEN concept Genome Center, Dresden, Germany. [19]Institut Universitaire de France, Paris, France. [20]Department of Mammalogy, Division of Vertebrate Zoology, American Museum of Natural History, New York, NY, USA. [21]The Vertebrate Genome Laboratory, The Rockefeller University, New York, NY, USA. [22]Department of Bioengineering and Therapeutic Sciences, University of California San Francisco, San Francisco, CA, USA. [23]Institute for Human Genetics, University of California San Francisco, San Francisco, CA, USA. [24]Environment Authority, Al Khuwair, Oman. [25]Center of Animal Behavior, Smithsonian Tropical Research Institute, Balboa, Panama. [26]University of California Santa Cruz, Santa Cruz, CA, USA. [27]Ecology and Evolutionary Biology, University of Toronto, Toronto, Ontario, Canada. [28]Department of Zoology, National Museum, Prague, Czech Republic. [29]Department of Zoology, Faculty of Science, Charles University, Prague, Czech Republic. [30]Biodetics Data Solutions, Guelph, Ontario, Canada. [31]Ecological and Regulatory Solutions, Inc., University of Guelph, Guelph, Ontario, Canada. [32]SOH Conservación, Santo Domingo, Dominican Republic. [33]Department of Medicine, KCVI, Oregon Health & Science University, Portland, OR, USA. [34]Department of Molecular and Medical Genetics, Oregon Health & Science University, Portland, OR, USA. [35]Division of Genetics, Oregon National Primate Research Center, Beaverton, OR, USA. [36]New Cultivar Innovation, New Zealand Institute for Bioeconomy Science Limited, Auckland, New Zealand. [37]Programme for Emerging Infectious Diseases, Duke-NUS Medical School, Singapore, Singapore. [38]Max Planck Institute of Animal Behavior, Radolfzell, Germany. [39]University of Konstanz, Konstanz, Germany. [40]Institute for Neurobiology, University of Tübingen, Tübingen, Germany. [41]Department of Environmental Science, School of Science, University of Namibia, <City>, Namibia. [42]National Museum of Namibia, Windhoek, Namibia. [43]Department of Ecology and Evolutionary Biology, University of Arizona, Tucson, AZ, USA. [44]Veterinary Integrative Biosciences, Texas A&M University, College Station, TX, USA. [45]Center for Comparative Genomics, Texas A&M AgriLife Research, College Station, TX, USA. [46]Department of National Parks and Wildlife, Research and Development Section, Lilongwe, Malawi. [47]Department of Evolutionary Ecology, National Museum of Natural Sciences, CSIC, Madrid, Spain. [48]Department of Anatomy, Faculty of Biomedical Sciences, University of Otago, Otago, New Zealand. [49]Instituto de Investigación de Recursos Biológicos Alexander von Humboldt, Bogota, Colombia. [50]Negaunee Integrative Research Center, Field Museum of Natural History, Chicago, IL, USA. [51]Association Vahatra, Antananarivo, Madagascar. [52]Paratus Sciences, New York, NY, USA. [53]Department of Biological Sciences, California State University Stanislaus, Turlock, CA, USA. [54]Laboratorio de Bioconservación y Manejo, Escuela Nacional de Ciencias Biológicas, IPN, Mexico City, Mexico. [55]Department of Genetics, University of Granada, Granada, Spain. [56]Bioinformatics Laboratory, Biotechnology Institute & Biomedical Research Centre (CIBM), Granada, Spain. [57]Institute of Cell Biology and Neuroscience, Faculty of Biosciences, Goethe University Frankfurt, Frankfurt, Germany. [58]Department of Biological Sciences, Fairleigh Dickinson University, New Jersey, NJ, USA. [59]Cobra Collective Guyana, Georgetown, Guyana. [60]Hughes Medical Institute, Chevy Chase, MD, USA. [61]Amazon Conservation Team, Paramaribo, Suriname. [62]Institute for Biology, Humboldt-Universität zu Berlin, Berlin, Germany. [63]Museum für Naturkunde-Leibniz Institute for Evolution and Biodiversity Science, Berlin, Germany. [64]Department of Ecology and Evolutionary Biology, University of California, Los Angeles, CA, USA. [65]Department of Biology, University of Vermont, Vermont, USA. [66]Paul G. Allen School for Global Health, College of Veterinary Medicine, Washington State University, Pullman, WA, USA. [67]Julie Ann Wrigley Global Futures Laboratory, Walton Center for Planetary Health, Arizona State University, Tempe, AZ, USA. [68]Department of Molecular Medicine, Aarhus University Hospital (AUH), Aarhus, Denmark. [69]Department of Clinical Medicine, Aarhus University, Aarhus, Denmark. [70]Bragato Research Institute, Lincoln, New Zealand. [71]Science and Research Directorate, Department of Conservation, Wellington, New Zealand. [72]Medical Affairs Organization, Illumina, San Diego, CA, USA. [73]Centro de Investigaciones Tropicales, Universidad Veracruzana, Veracruz, Mexico. [74]Institute of Evolutionary Ecology and Conservation Genomics, Ulm University, Ulm, Germany. [75]Laboratory of Virology, Division of Intramural Research, National Institute of Allergy and Infectious Diseases, <City>, MT, USA. [76]Universite de Caen Normandie, Universite Rouen Normandie, INSERM, Caen, France. [77]Department of Forests, Ministry of Agriculture Rural Development and Environment, <City>, Cyprus. [78]Department of Wildlife and Range Management, Kwame Nkrumah University of Science and Technology, Kumasi, Ghana. [79]Bina Hill Institute Youth Learning Centre, Bina Hill, Guyana. [80]Wildlife Conservation Society, Health Program, Bronx, NY, USA. [81]Wildlife Health Program, Wildlife Conservation Society, Brazzaville, Republic of the Congo. [82]School of Biological Sciences, University of Auckland, Auckland, New Zealand. [83]West German Genome Center (WGGC), Medical Faculty and University Hospital Düsseldorf, Heinrich Heine University Düsseldorf, Düsseldorf, Germany. [84]Biological and Medical Research Center (BMFZ), Medical Faculty and University Hospital Düsseldorf, Heinrich Heine University Düsseldorf, Düsseldorf, Germany. [85]Department of Veterinary and Biomedical Sciences,

College of Veterinary Medicine, University of Minnesota, St. Paul, MN, USA. [86]School of Life and Health Sciences, University of Nicosia, Nicosia, Cyprus. [87]Escuela de Ciencias e Ingeniería, Universidad del Rosario, Bogota, Colombia. [88]School of Biology and Center for Research in Biodiversity and Tropical Ecology (CIBET), University of Costa Rica, San Jose, Costa Rica. [89]Department of Natural Sciences and Mathematics, Pontificia Universidad Javeriana Cali, Cali, Colombia. [90]Environmental Management Consultants Guyana, Ogle, East Coast Demerara, Guyana. [91]Rupununi Wildlife Research Unit, Lethem, Guyana. [92]School of Biological and Behavioural Sciences, Queen Mary University of London, London, UK. [93]Institute of Biology, Freie Universitat Berlin, Berlin, Germany. [94]Wildconscience, Kralendijk, Bonaire, Netherlands. [95]CARMABI Caribbean Research and Management of Biodiversity, Willemstad, Curaçao. [96]Princess Maha Chakri Sirindhorn Natural History Museum, Prince of Songkla University, Songkhla, Thailand. [97]Independent Wildlife Consultant, Muscat, Oman. [98]Bat Conservation Research Lab, Milner Research Institute, University of Bath, Bath, UK. [99]African Bat Conservation, Lilongwe, Malawi. [100]Department of Integrative Biology, University of California Berkeley, Berkeley, CA, USA. [101]Biodiversity Institute, University of Kansas, Lawrence, KS, USA. [102]Department of Ecology & Evolutionary Biology, University of Kansas, Lawrence, KS, USA. [103]Czech Academy of Sciences, Institute of Vertebrate Biology, Brno, Czech Republic. [104]Department of Biology, Pennsylvania State University, University Park, PA, USA. [105]Freshwater Quality Monitoring Division, Science and Technology Branch, Environment and Climate Change Canada, Burlington, Ontario, Canada. [106]AEWC Ltd/BatCRU, Fittleworth, UK. [107]Department of Bioinformatics and Genomics, University of North Carolina, Charlotte, NC, USA. [108]Otago Genomics Facility, University of Otago, Dunedin, New Zealand. [109]State Key Laboratory of Virology and Biosafety, College of Life Sciences, Wuhan University, Wuhan, China. [110]Consortium on Inter-Disciplinary Environmental Research, Institute for Advanced Computational Science, Stony Brook University, New York, NY, USA. [111]Present address: The City College of New York, New York, NY, USA. [112]These authors contributed equally: Yan Liang, William R. Thomas, Evgeny V. Leushkin, Francisco X. Castellanos, Denis M. Larkin, Tom Brown. [113]These authors jointly supervised this work: Bastian Fromm, Suzanne J. Hand, Zixia Huang, Graham M. Hughes, Matthew F. Jones, Burton K. Lim, Meike Mai, Eugene W. Myers, Martin Pippel, Sebastien J. Puechmaille, Nancy B. Simmons. ✉e-mail: david.4.ray@gmail.com; scv1@st-andrews.ac.uk; liliana.davalos@stonybrook.edu; michael.hiller@senckenberg.de; emma.teeling@ucd.ie

Reporting summary

Further information on research design is available in the Nature Portfolio Reporting Summary linked to this article.

Data availability

Dataset are available on Dryad (https://doi.org/10.5061/dryad.1rn8pk187). All genome accession numbers and/or Bioproject IDs are listed in Supplementary Table 1.1.

Code availability

Custom scripts used for data analysis are available on GitHub[68] (https://github.com/Bat1K-21families/21families-analyses).

68. Morales, A. Bat1K 21families: analyses, code, and contributors. *GitHub* https://github.com/Bat1K-21families/21families-analyses (2026).
69. Tian, S. et al. Comparative analyses of bat genomes identify distinct evolution of immunity in Old World fruit bats. *Sci. Adv.* **9**, eadd0141 (2023).
70. Simmons, N. B. et al. The genome sequence of Molossusnigricans (Chiroptera, Molossidae; Miller, 1902). *Wellcome Open Res.* **8**, 198 (2023).
71. Curti, J. et al. A genome assembly of the Yuma myotis bat, *Myotis yumanensis*. *J. Hered.* https://doi.org/10.1093/jhered/esad053 (2023).
72. Capel, S. L. R. et al. Reference genome of Townsend's big-eared bat, *Corynorhinus townsendii*. *J. Hered.* **115**, 203–211 (2024).
73. Geng, Y. et al. A chromosome-level genome assembly of an avivorous bat species (*Nyctalus aviator*). *Sci. Data* **11**, 480 (2024).
74. Ruedi, M. et al. The genome sequence of the Soprano Pipistrelle, *Pipistrellus pygmaeus* (Leach, 1825). *Wellcome Open Res.* **8**, 360 (2023).
75. van der Kooij, J. et al. The genome sequence of the northern bat, *Eptesicus nilssonii* (Keyserling & Blasius, 1839). *Wellcome Open Res.* **8**, 362 (2023).
76. Webster, C. F. et al. The genome sequence of *Tadarida brasiliensis* I. Geoffroy Saint-Hilaire, 1824 [Molossidae; Tadarida]. *Wellcome Open Res.* **9**, 98 (2024).
77. Driller, M. et al. A haplotype-resolved reference genome of a long-distance migratory bat, *Pipistrellus nathusii* (Keyserling & Blasius, 1839). *DNA Res.* **31**, dsae018 (2024).
78. Ruedi, M. et al. The genome sequence of Daubenton's bat, *Myotis daubentonii* (Kuhl, 1817). *Wellcome Open Res.* **9**, 107 (2024).
79. Millar, A. et al. The genome sequence of the brown long-eared bat, *Plecotus auritus* (Linnaeus 1758). *Wellcome Open Res.* **9**, 246 (2024).
80. Alvarez van Tussenbroek, I. et al. The genome sequence of *Rhynchonycteris naso*, Peters, 1867 (Chiroptera, Emballonuridae, Rhynchonycteris). *Wellcome Open Res.* **9**, 361 (2024).
81. Vandendriessche, B. et al. The genome sequence of the particolored bat, *Vespertilio murinus* Linnaeus, 1758. *Wellcome Open Res.* **9**, 403 (2024).
82. Simmons, N. B. et al. The genome sequence of *Molossus alvarezi* González-Ruiz, Ramírez-Pulido and Arroyo-Cabrales, 2011 (Chiroptera, Molossidae). *Wellcome Open Res.* **9**, 522 (2024).
83. Wang, Z. et al. Comparative analysis of chromosome-level genomes provides insights into chromosomal evolution in Chiroptera. *Integr. Zool.* **20**, 1185–1203 (2025).
84. Vazquez, J. M. et al. Extensive longevity and DNA virus-driven adaptation in nearctic *Myotis* bats. Preprint at *bioRxiv* https://doi.org/10.1101/2024.10.10.617725 (2024).
85. Ryan, H. et al. The genome sequence of the whiskered bat, *Myotis mystacinus* (Kuhl, 1817). *Wellcome Open Res.* **9**, 684 (2024).
86. Tian, S. et al. Comparative genomics provides insights into chromosomal evolution and immunological adaptation in horseshoe bats. *Nat. Ecol. Evol.* **9**, 705–720 (2025).
87. Simmons, N. B. et al. The genome sequence of *Glossophaga mutica* (Chiroptera, Phyllostomidae, Glossophaginae; Merriam, 1898). *Wellcome Open Res.* **10**, 174 (2025).
88. Simmons, N. B. et al. The genome sequence of *Artibeus lituratus* (Chiroptera, Phyllostomidae, Stenodermatinae; Olfers, 1818). *Wellcome Open Res.* **10**, 170 (2025).
89. Tian, S., Zhang, L. & Zhao, H. Chromosome-level genome assembly of the big-footed bat (*Myotis pilosus*). *Res. Sq.* https://doi.org/10.21203/rs.3.rs-7561642/v1 (2025).
90. Liu, S. Integrated genomics and transcriptomics reveal mechanisms of extreme dietary adaptation in vampire bats. Preprint at *bioRxiv* https://doi.org/10.64898/2026.07.24.740446 (2026).

Acknowledgements We thank all members of the Bat1K consortium for their contributions to coordinating and advancing this work; extend our appreciation to all fieldworkers, without whose efforts in sample collection and stewardship this research and the resulting genomes would not have been possible; Ngāti Rangi iwi and the New Zealand Department of Conservation for support; R. Foo for providing the *Eonycteris* sample; A. Cuervo for logistical support during the 2019 Colciencias Expedition in Colombia; R. Page and G. Cohen of the Smithsonian Tropical Research Institute for contributions to sample collection in Panama; and the Wellcome Sanger Institute Data Release Team for their support with raw data and genome assembly organization and submission. Fieldwork support included Environmental Services & Support and SRK Consulting (Suriname); the Royal Ontario Museum Governors (Guyana, Suriname, Vietnam, Malaysia, Dominican Republic, Nevis, Bonaire and Curaçao); Colciencias Colombia Bio for work in Colombia; and Ecuambiente Consulting Group for work in Ecuador. We are grateful to the Genome Technology Center (RGTC) at Radboudumc for access to the Sequencing Core Facility (Nijmegen, the Netherlands) and the DRESDEN-concept Genome Center, supported by the DFG Research Infrastructure Program (project 407482635) and as part of the Next Generation Sequencing Competence Network (project 423957469). Computational resources were provided by the Zentrum für Informations und Medientechnologie, particularly the HPC team, at Heinrich Heine University; Stony Brook Research Computing and Cyberinfrastructure and the Institute for Advanced Computational Science, through access to the SeaWulf computing system—made possible by grants from the US National Science Foundation (awards 1531492 and 2215987) and matching funds from the Empire State Development's Division of Science, Technology and Innovation (NYSTAR) programme (contract C210148); the University of Otago, New Zealand; and Genomics Aotearoa, which provided both computational resources and funding support.

Author contributions This study was conceptualized and led by the five corresponding authors: E.C.T., M.Hiller, L.M.D., S.C.V. and D.A.R. who led the scientific direction, manuscript writing and editing. Together with the corresponding authors, 18 co-authors led the data analyses and interpretation detailed in the Supplementary Notes and contributed to writing and editing: A.E.M., Y.L., W.R.T., E.V.L., F.X.C., D.M.L., T.B., B.F., S.J.H., Z.H., G.M.H., M.F.J., B.K.L., M.Mai, E.W.M., M.Pippel, S.J.P. and N.B.S. All authors had the opportunity to review and edit the manuscript. Z.A.A., I.A.V.T., D.V.A., L.M.A.H., P.B., A.V.B., J.B., N.C., W.O.Y.C., L.M.D., D.K.N.D., A.D., D.E., M.D.E., I.G., A.M.G., S.M.G., E.G.G., L.H., M.R.d.W., D.M.J., S.A.J., M.K., J.E.K., M.E.L., M.L., B.K.L., B.D.L., L.L., V.J.M., N.N., H.N., E.E.N., Z.N., S.H.O., A.O., B.A.O., J.O., K.L.P., M.Pieri, S.J.P., P.P.-S., D.A.R., B.R.-H., I.R., S.J.R., C.S., S.N.S., N.B.S., A.S., E.L.S., P.H.S., R.M.T., N.S.U., J.M.V., S.C.V., L.-F.W., L.C.W., D.W., Y.W., L.R.Y., H.Z., J.L.E., S.J.E., J.F., M.A.G., T.W.H., M.C.M.G., M.N., D.R., F.S., P.S., W.O.M., E.C.T., M.Hiller, M.Mai and P.V. acquired samples and data. S.W., D.W.M., C.G., A.B.H., A.M.G., D.K.L., E.H., F.J.P.-L., J.I.C., J.E.G., K.A.N., L.C., M.Meyer, M.W.G., M.Z., N.J.G., N.Z., W.O.Y.C., W.S.P., Y.G., S.S., N.A., B.P.O., L.-F.W., S.C.V., E.C.T. and M.Hiller performed genome sequencing. T.B., E.V.L., M.Pippel, T.S., L.A.L.A., K.M., S.T., B.K., G.F., E.D.J., L.U., E.W.M., S.C.V., E.C.T., M.B., M.Hiller and B.P.O. conducted the genome assembly. A.E.M., E.V.L., D.A.R. and M.Hiller performed the assembly statistics. A.E.M., A.G.-I., Y.V.M., L.H., S.L., D.-G.K., E.V.L. and M.Hiller conducted genome annotation and pairwise genome alignments. D.A.R. and L.M.D. performed the transposable element annotation. B.F., Z.H., S.P., M.U., M.Mai and S.C.V. conducted the microRNA analyses. A.E.M., E.V.L., F.X.C., D.A.R. and M.Hiller performed the multiple genome alignments. A.E.M., E.C.T., M.Hiller, A.G.-I., G.M.H., S.J.P., Y.L., N.M.F. and W.J.M. undertook the phylogenomics. M.Prylutskyi, A.E.M., M.Hiller, H.A.L. and D.M.L. performed the ancestral karyotype reconstruction. W.R.T., M.F.J., F.X.C., G.M.H., S.J.H., N.B.S., L.M.D. and E.C.T. contributed fossils, total evidence and node divergence times, and biogeography. A.B.H., T.B., P.D., G.F., A.G.-I., J.G., M.F.J., B.K., M.E.L., E.V.L., Y.L., M.Mai, Y.V.M., A.E.M., M.Pippel, T.S., N.B.S., W.R.T., M.Muffato, G.Q., L.U., E.C.T., M.Hiller, L.M.D., S.C.V. and D.A.R. curated the data and performed the archving.

Funding This work was supported by the Max Planck Society; the LOEWE-Centre for Translational Biodiversity Genomics (TBG) funded by the Hessen State Ministry of Higher Education, Research and the Arts (LOEWE/1/10/519/03/03.001(0014)/52); the German Research Foundation (DFG) through grants HI1423/5-1 and HI1423/6-1; DFG grant SEQ1201/SO 428/17-1 as part of the DFG sequencing call 2.2 (awarded to S.S. and C. Drosten); the European Research Council (ERC) under the European Union's Horizon 2020 and Horizon Europe programmes through awards: BATPROTECT ERC-2023-SyG 101118919 (awarded to E.C.T., M.Hiller and L.-F.W.); ERC Consolidator Grant BATSPEAK 101001702 (awarded to S.C.V.); and ERC GA 804352 (awarded to M.K.). This work also received support from the UKRI Future Leaders Fellowship (MR/T021985/1 awarded to S.C.V.); Science Foundation Ireland (Future Frontiers (19/FFP/6790, awarded to E.C.T.) and 18/CRT/6214); the Irish Research Council Laureate Award (IRCLA/2022/3212 awarded to E.C.T.); the University College Dublin Ad Astra Programme (awarded to G.M.H.); the Wellcome Trust awards 220540/Z/20/A (Sanger Core), 218328/Z/19/Z (DToL discretionary award) and 226458/Z/22/Z (DToL bridge award); the Institut Universitaire de France, including a Junior Chair (awarded to S.J.P.) the Field Museum of Natural History (Madagascar fieldwork); the Genetic Resources Collection at the Natural Science Research Laboratory of the Museum of Texas Tech University; the High Performance Computing Center at Texas Tech University; the Dávalos laboratory, supported by the Stony Brook University Presidential Innovation and Excellence Award and a charitable donation from P. Hurst-Della Pietra; the Singapore National Research Foundation (NRF-CRP10-2012-05); the R&D Program of Guangzhou National Laboratory (SRPG22-001); the NOMIS Fellowship Program at STRI; and Genomics Aotearoa. We also acknowledge support from the DFG Research Infrastructure West German Genome Center (project 407493903). The National Science Foundation (NSF DEB-0344430) provided support from the DFG Research Infrastructure West German Genome Center (project 407493903) for work in China. This research was further supported by the US National Science Foundation (IOS 2031906, 2032063 and 2217296; OISE 2020577; and PRFB 2010884, 2109915 and 2515340); the National Human Genome Research Institute (R01HG012396); and the US National Institutes of Health (NIH), including NIGMS MIRA 5R35GM142677, and IRACDA K12GM081266, R35GM142916, K99AG088361 and T32AG000266. Additional support was provided by the Intramural Research Program of the NIH, whose authors contributed as part of their official duties as US Government employees. The findings and conclusions do not necessarily reflect the views of the NIH or HHS. We also acknowledge support from the Ministry of Culture of the Czech Republic (DKRVO 23272/2024–2028/6.I.c); the Ministry of Education, Youth and Sports of the Czech Republic (LTAUSA19147); the Thailand Research Fund (DBG6180028); the Ciencias de Frontera programme (15307); and personal funding provided to individual contributors.

Competing interests The authors declare no competing interests.

Additional information

Supplementary information The online version contains supplementary material available at https://doi.org/10.1038/s41586-026-11007-3.

Correspondence and requests for materials should be addressed to David A. Ray, Sonja C. Vernes, Liliana M. Dávalos, Michael Hiller or Emma C. Teeling.

Peer review information *Nature* thanks Yafei Mao who co-reviewed with Zikun Yang; Josefin Stiller and Gerald Wilkinson for their contribution to the peer review of this work. Peer reviewer reports are available.

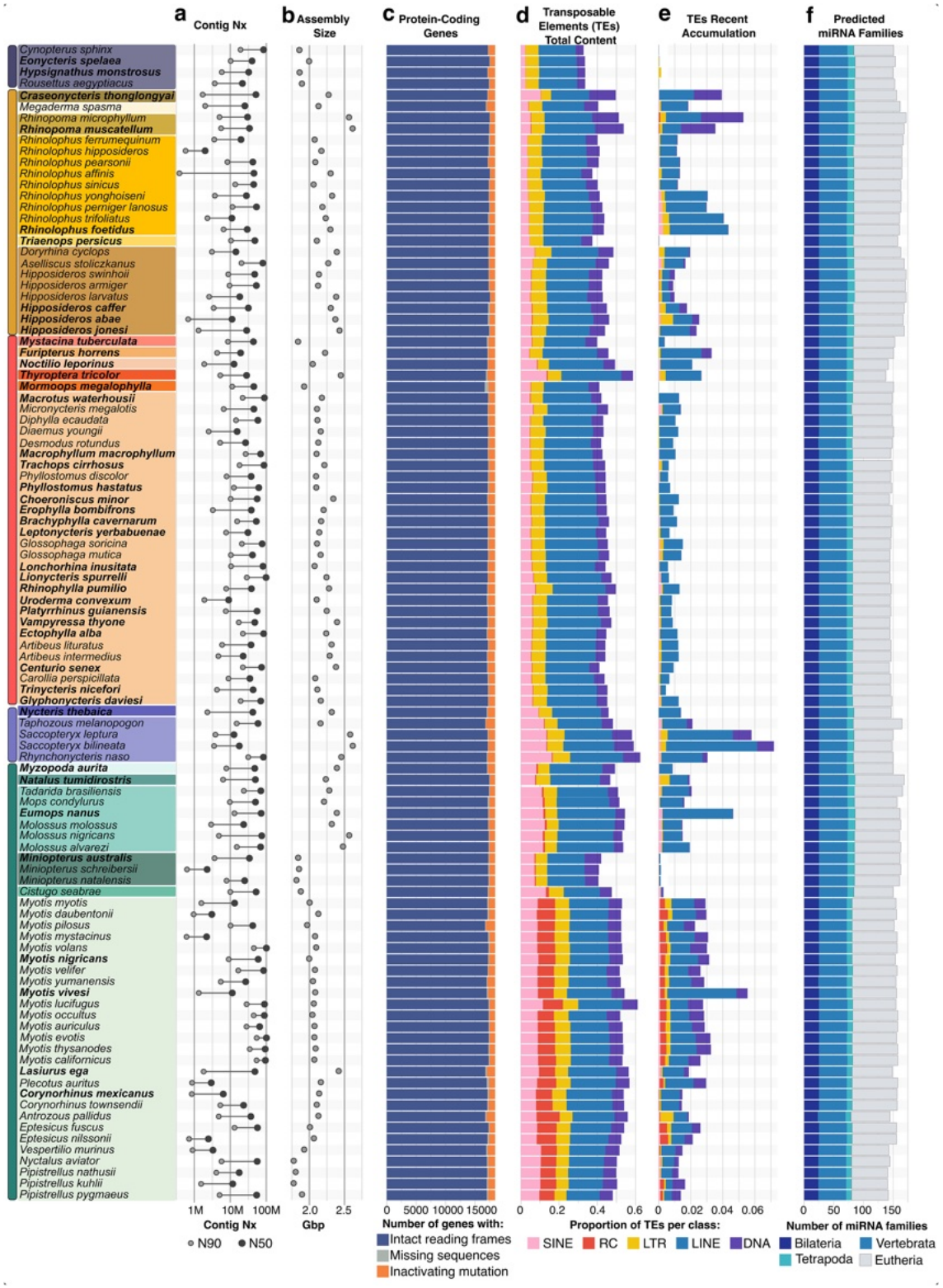

Extended Data Fig. 1 | See next page for caption.

Extended Data Fig. 1 | Summary statistics of all 103 bat genome assemblies and annotations. (**a**) Contig N50 and N90 values, indicating that 50/90 percent of the assembly consists of contigs of at least that size. New genomes have contig N50 values ranging from 6.4 to 102 Mb and all have chromosome-level scaffolds. (**b**) Assembly sizes. (**c**) Classification of 18,430 ancestral placental mammalian genes per assembly inferred by TOGA[33]. Our new assemblies contain at least 16,652 genes and on average 17,138 genes with intact reading frames. (**d**) Total transposable element (TE) representation in each assembly from all TE classes. (**e**) Recent TE accumulation in each assembly, defined as TEs with <10% divergence from the relevant consensus sequence. Assuming an average mammalian mutation rate of 2.2e-9, this would suggest accumulation less than ~45.5 mya. (**f**) Number of microRNA families predicted using MirMachine. The four categories (Bilateria, Vertebrata, Tetrapoda, and Eutheria) correspond to the phylogenetic levels at which each microRNA originated. Species are sorted according to the T2 topology (neutral windows, X chromosomes, and XLRD) and color-coded per family and superfamily as in Fig. 1). New assemblies are highlighted in bold. Together with existing high-quality assemblies of bats[5,6,25,69–90] these assemblies cover 103 bat species. Across the combined dataset, TOGA detected an average of 17,165 ancestral genes with intact reading frames and compleasm reported a mean gene completeness of 98.77% (Supplementary Table 4.1), indicating a consistently high quality.

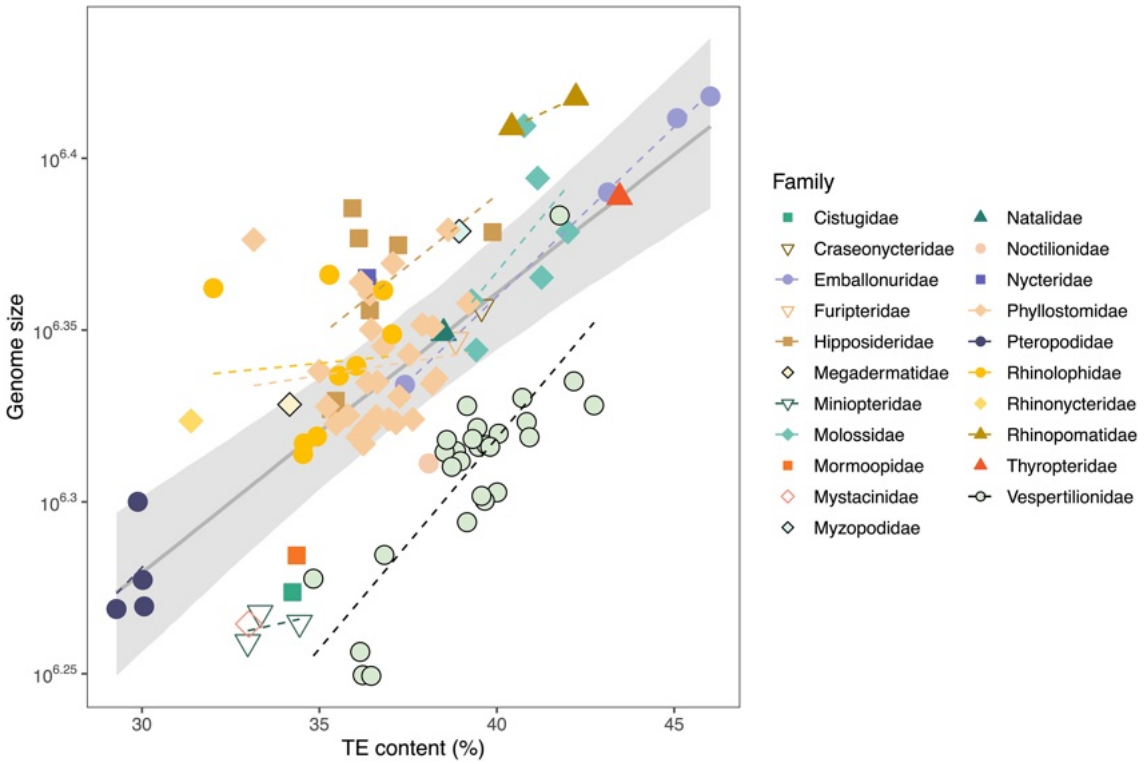

Extended Data Fig. 2 | Genome assembly size as function of TE content with colors indicating the corresponding bat family. The relationship shown corresponds to the parameters for the model in Supplementary Table 6.2.

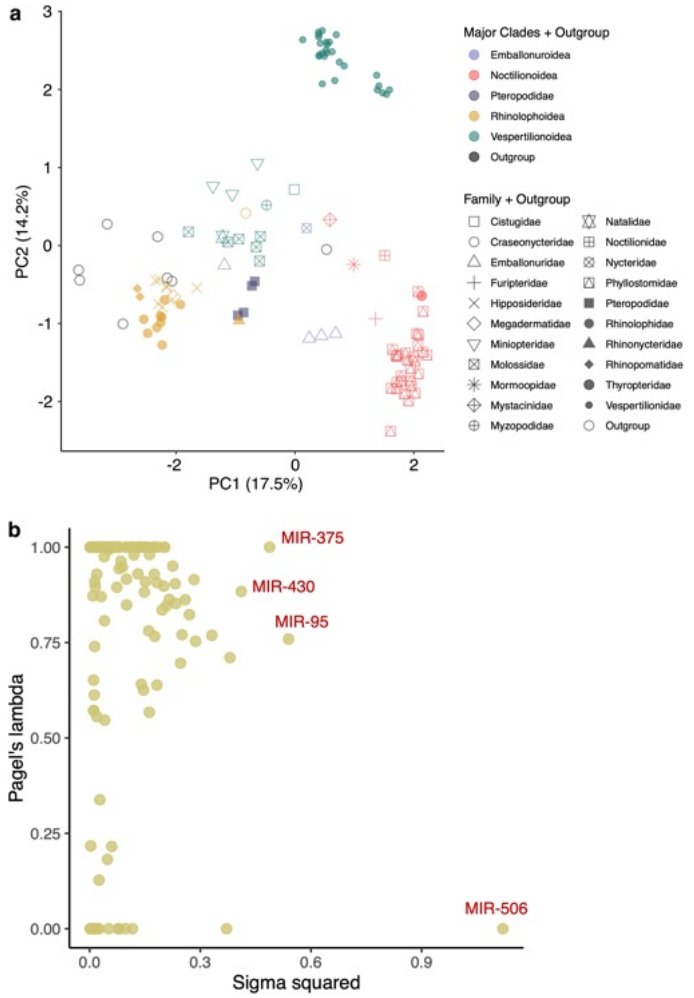

Extended Data Fig. 3 | Copy number analyses of 188 microRNA families across 103 bat species. (**a**) Principal Component Analysis (PCA) of microRNA family copy numbers across 103 bat species and 8 outgroup species. Colors represent the five major bat clades plus the outgroup, while shapes indicate the 21 bat families and the outgroup. (**b**) Evolutionary analyses of microRNA family copy number across 103 bat species and 8 outgroup species. Pagel's lambda quantifies the strength of phylogenetic signal in copy number distribution, ranging from 0 (no phylogenetic signal) and 1 (variation fully explained by phylogeny), while σ^2 reflects the rate of copy number evolution under a Brownian motion model, with higher values indicating faster rates of copy number change.

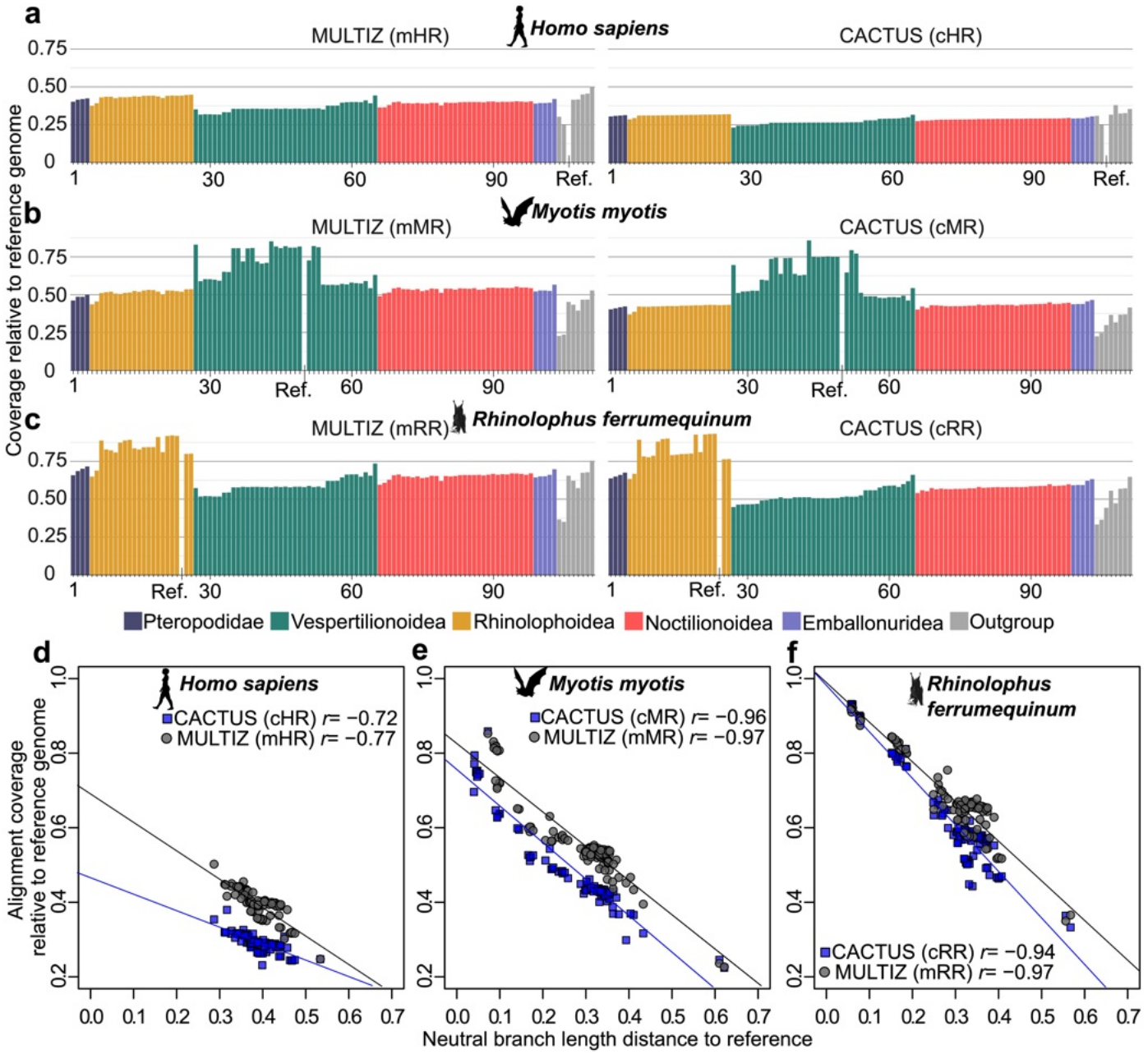

Extended Data Fig. 4 | Evolutionary distance to the reference is a major determinant of whole genome alignment coverage in MULTIZ and CACTUS alignments. (**a**–**c**), Genome alignment coverage for each reference species and alignment method. Coverage was calculated as the fraction of the reference genome covered by alignment blocks for each query species. Results are shown for three reference-based MULTIZ alignments (left) and three projected CACTUS alignments (right) generated from 103 bat species and eight mammalian outgroups. Reference or projected genomes are *Homo sapiens* (**a**), the yangochiropteran bat *Myotis myotis* (**b**), and the yinpterochiropteran bat *Rhinolophus ferrumequinum* (**c**). Alignments are abbreviated as mHR (MULTIZ *Homo* reference), mMR (MULTIZ *Myotis* reference), mRR (MULTIZ *Rhinolophus* reference), cHR (CACTUS *Homo* reference), cMR (CACTUS *Myotis* reference), and cRR (CACTUS *Rhinolophus* reference). Bars represent alignment coverage for each genome, grouped and colour-coded by bat superfamily or outgroup; and ordered from lowest to highest coverage as is provided in Supplementary Table 8.1. Species most closely related to the reference genome generally exhibit the highest alignment coverage. Coverage patterns are otherwise similar across Chiroptera and between alignment methods, although MULTIZ consistently yields slightly higher coverage than CACTUS for all three references. The higher coverage observed in MULTIZ likely reflects the use of sensitive LASTZ parameters and RepeatFiller during alignment construction (Supplementary Note 5). (**d**–**f**), Relationship between alignment coverage and evolutionary distance to the reference genome. Neutral branch length (measured as substitutions per site for fourfold-degenerate sites; Supplementary Note 9) between the reference and each query species is plotted against alignment coverage. Strong negative correlations were observed for all three reference genomes (*Homo sapiens*, **d**; *Myotis myotis*, **e**; *Rhinolophus ferrumequinum*, **f**) and the two alignment methods, indicating that evolutionary distance is a major determinant of alignment coverage. For MULTIZ alignments, correlation coefficients from two-sided Pearson's test were mHR/mMR/mRR r(108) = −0.77/ −0.97/−0.97, with all p-values < 0.0001; while for CACTUS, they were mHR/mMR/mRR r(108) = −0.72/−0.96/−0.94, with all p-values < 0.0001. The silhouettes of *M. myotis* and *R. ferrumequinum* were vectorized by A.E.M. from illustrations by Fiona Reid. The silhouette of *H. sapiens* was created using PhyloPic (https://phylopic.org) under a Creative Commons licence CC0 1.0.

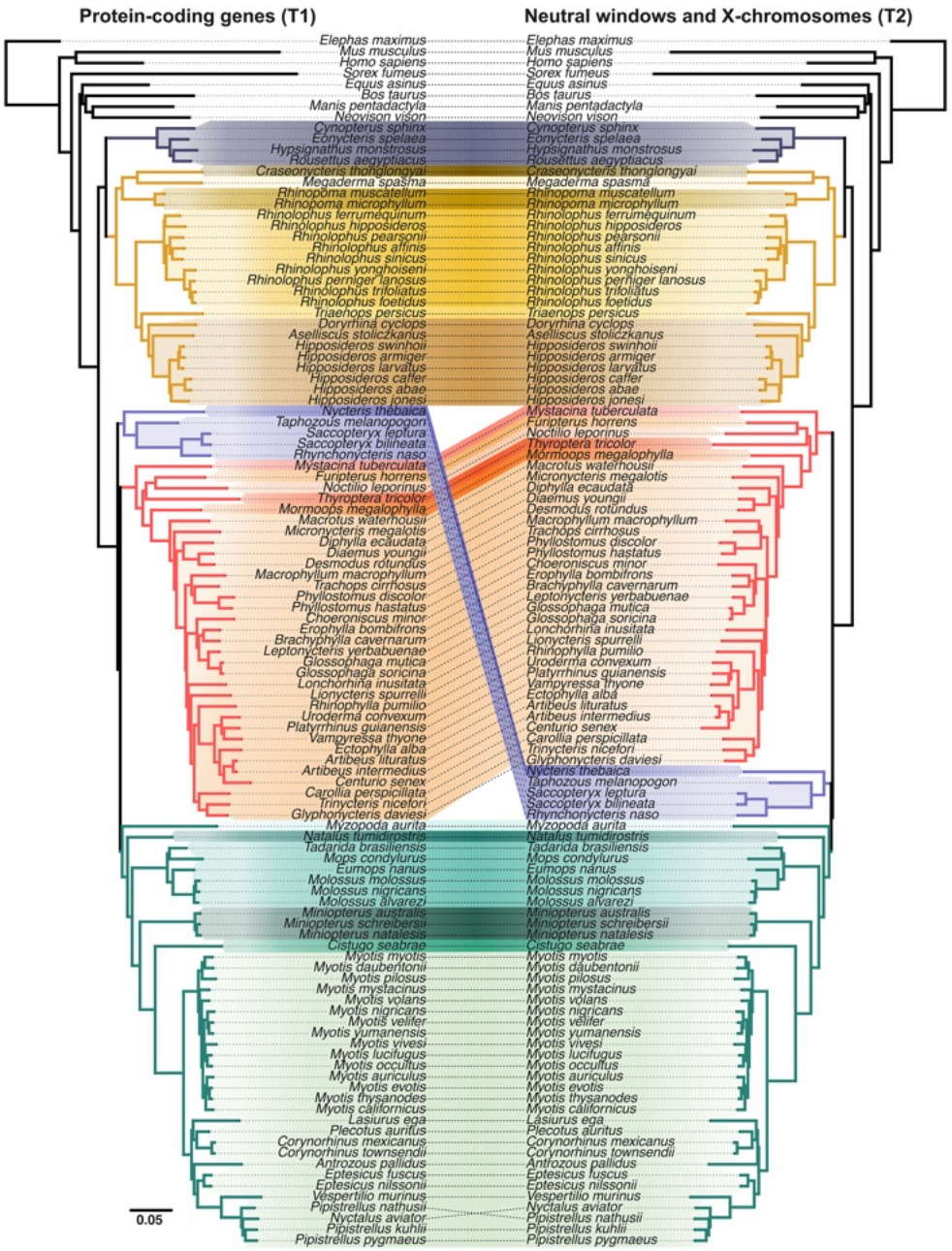

Extended Data Fig. 5 | Alternative phylogenetic placements of yangochiropteran superfamilies and *Pipistrellus nathusii*. (**Left**) Species trees inferred from 16750 protein-coding genes referred as (T1). (**Right**) Species trees inferred independently from intergenic neutral window regions extracted from the MULTIZ-human reference alignment and from the X chromosomes of each reference (*Homo, Myotis, Rhinolophus*), referred to as (T2). Branch lengths represent substitutions per neutral site and are color-coded per superfamily as in Fig. 1. Bands are color-coded per family and connect corresponding taxa between reconstructions.

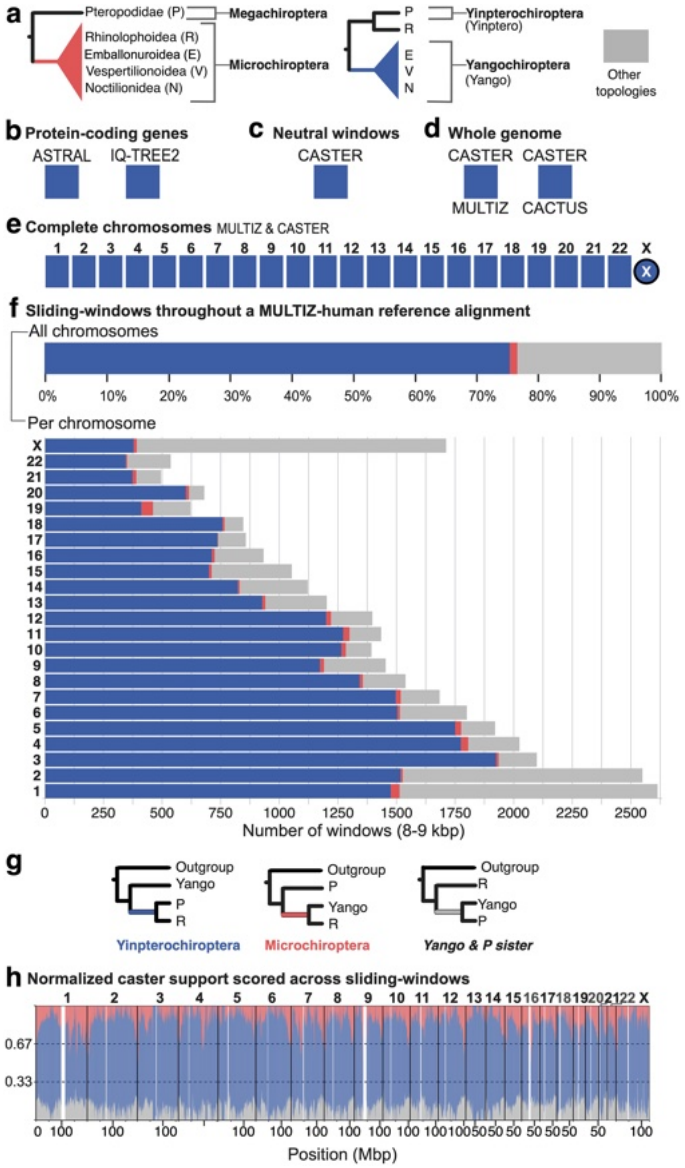

Extended Data Fig. 6 | All genome-wide analyses confirm the monophyly of the suborders Yinpterochiroptera and Yangochiroptera. (**a**) Hypotheses tested for higher-level suborder relationships among bats. (**b**) Results from protein-coding datasets inferred under coalescent and concatenated methods. (**c**) Analyses of neutral intergenic windows (≥500 bp) extracted from human-referenced alignment. (**d**) Whole-genome phylogenies based on two alignment methods (MULTIZ and CACTUS). (**e**) Chromosome-scale trees. (**f**) Non-overlapping sliding-window analyses; bars indicate the proportion of windows supporting each topology after excluding windows with >20% missing data. (**g**) Hypotheses tested for branch-specific support in CASTER analyses, and (**h**) normalized CASTER support scores for main and alternative topologies of each branch shown in (**g**), averaged over 5Mbp sliding windows for each chromosome. Regions missing from the alignment or showing low branch-specific coverage (for example, excessive gaps among quartets around a branch) are left blank. Sliding-window analyses were based on the MULTIZ human-reference alignment.

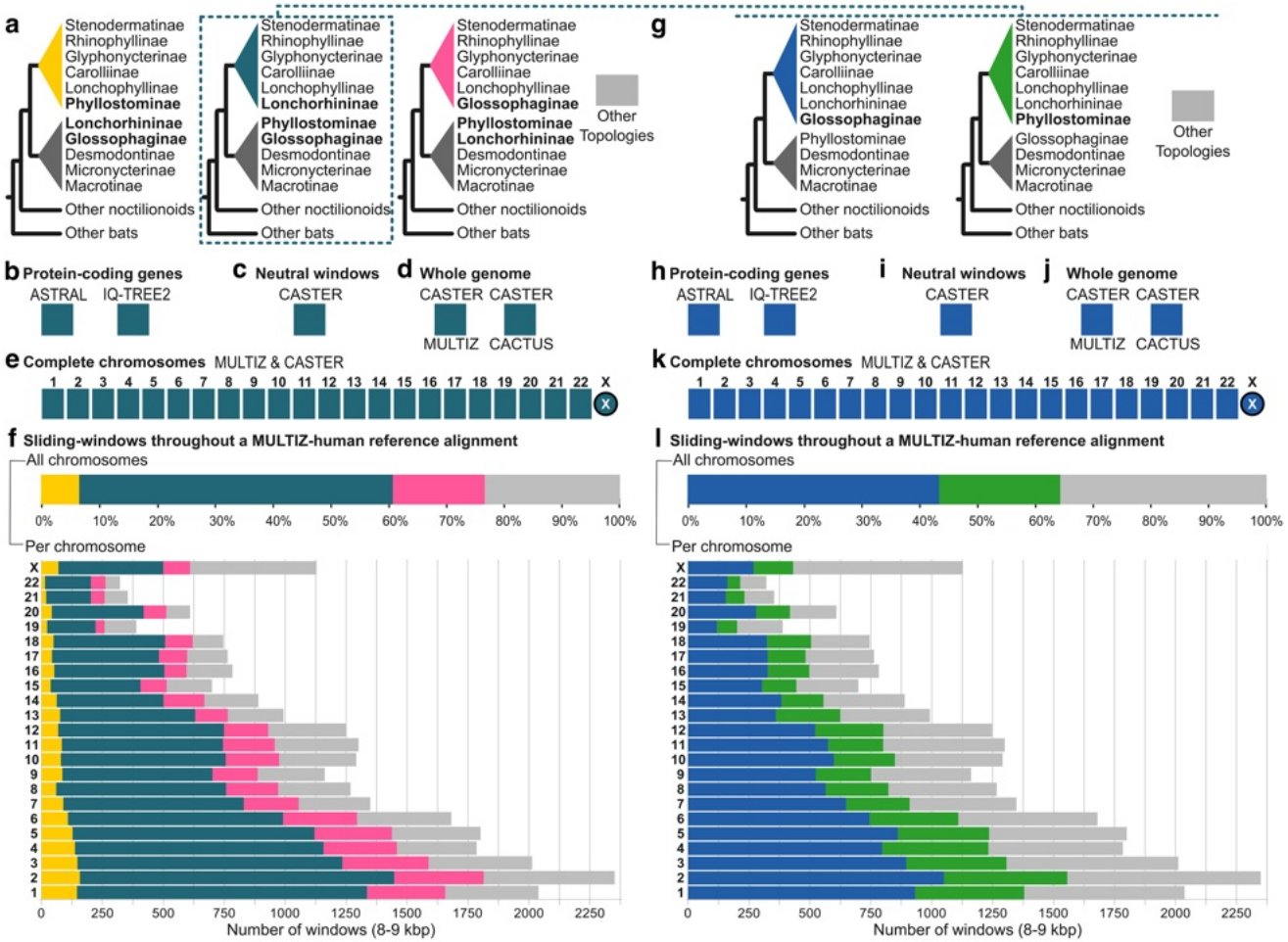

Extended Data Fig. 7 | Within the family Phyllostomidae, Lonchorhininae was consistently recovered across genomic data sets and inference methods as the earliest-diverging lineage within a clade comprising Stenodermatinae, Rhinophyllinae, Glyphonycterinae, Carolliinae and Lonchophyllinae, with Glossophaginae sister to this clade. (**a**,**g**) Hypotheses tested for higher-level relationships among phyllostomid subfamilies, (**b**,**h**) Results from protein-coding datasets inferred under coalescent and concatenated methods. (**c**,**i**) Analyses of neutral intergenic windows (≥ 500 bp) extracted from human-referenced alignment. (**d**,**j**) Whole-genome phylogenies based on two alignment methods (MULTIZ and CACTUS). (**e**,**k**) Chromosome-scale trees. (**f**,**l**) Non-overlapping sliding-window analyses; bars indicate the proportion of windows supporting each topology. To avoid including windows containing poorly aligned repetitive regions and frequent assembly gaps, we excluded windows with more than 20% missing data from the analyses. Sliding-window analyses were based on the MULTIZ human-reference alignment.

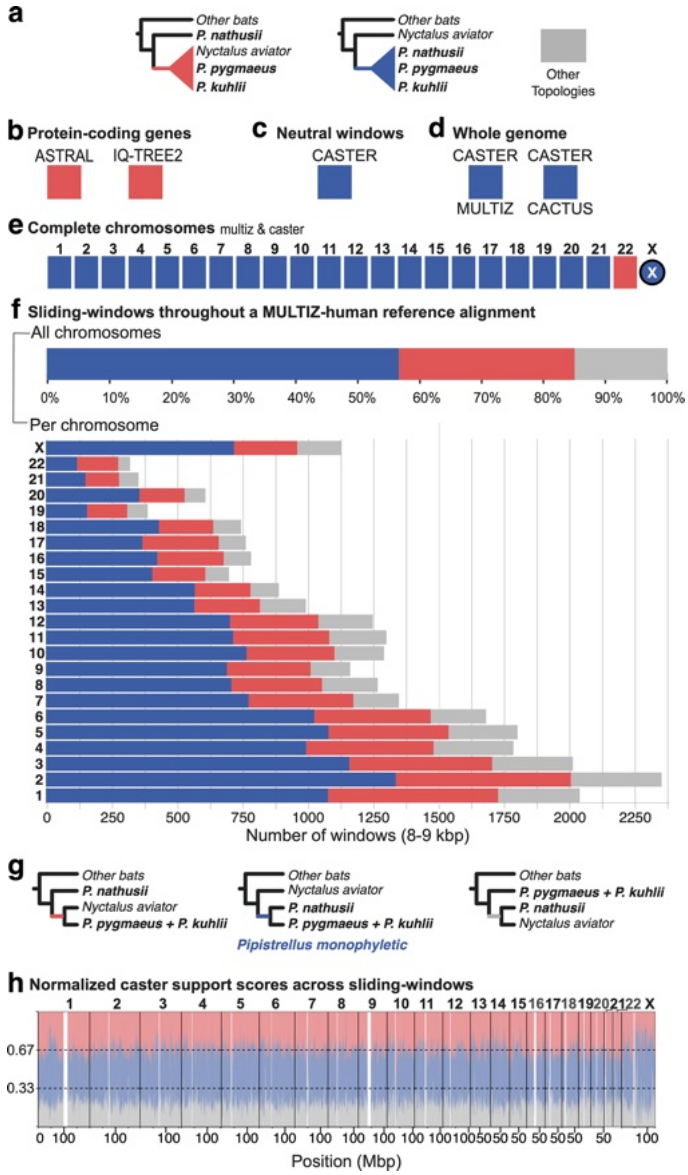

Extended Data Fig. 8 | Genome-wide analyses confirm the monophyly of the genus *Pipistrellus*. (**a**) Hypotheses tested for monophyly relationships among species of the genus *Pipistrellus* and *Nyctalus*. (**b**) Results from protein-coding datasets inferred under coalescent and concatenated methods. (**c**) Analyses of neutral intergenic windows (≥500 bp) extracted from human-referenced alignment. (**d**) Whole-genome phylogenies based on two alignment methods (MULTIZ and CACTUS). (**e**) Chromosome-scale trees. (**f**) Non-overlapping sliding-window analyses. (**g**) Branch support tested in CASTER analyses, and (**h**) normalized CASTER support scores for main and alternative topologies of each branch shown in (**g**), averaged over 5Mbp sliding windows for each chromosome. Regions missing from the alignment or showing low branch-specific coverage (for example, excessive gaps among quartets around a branch) are left blank. Sliding-window analyses were based on the MULTIZ human-reference alignment.

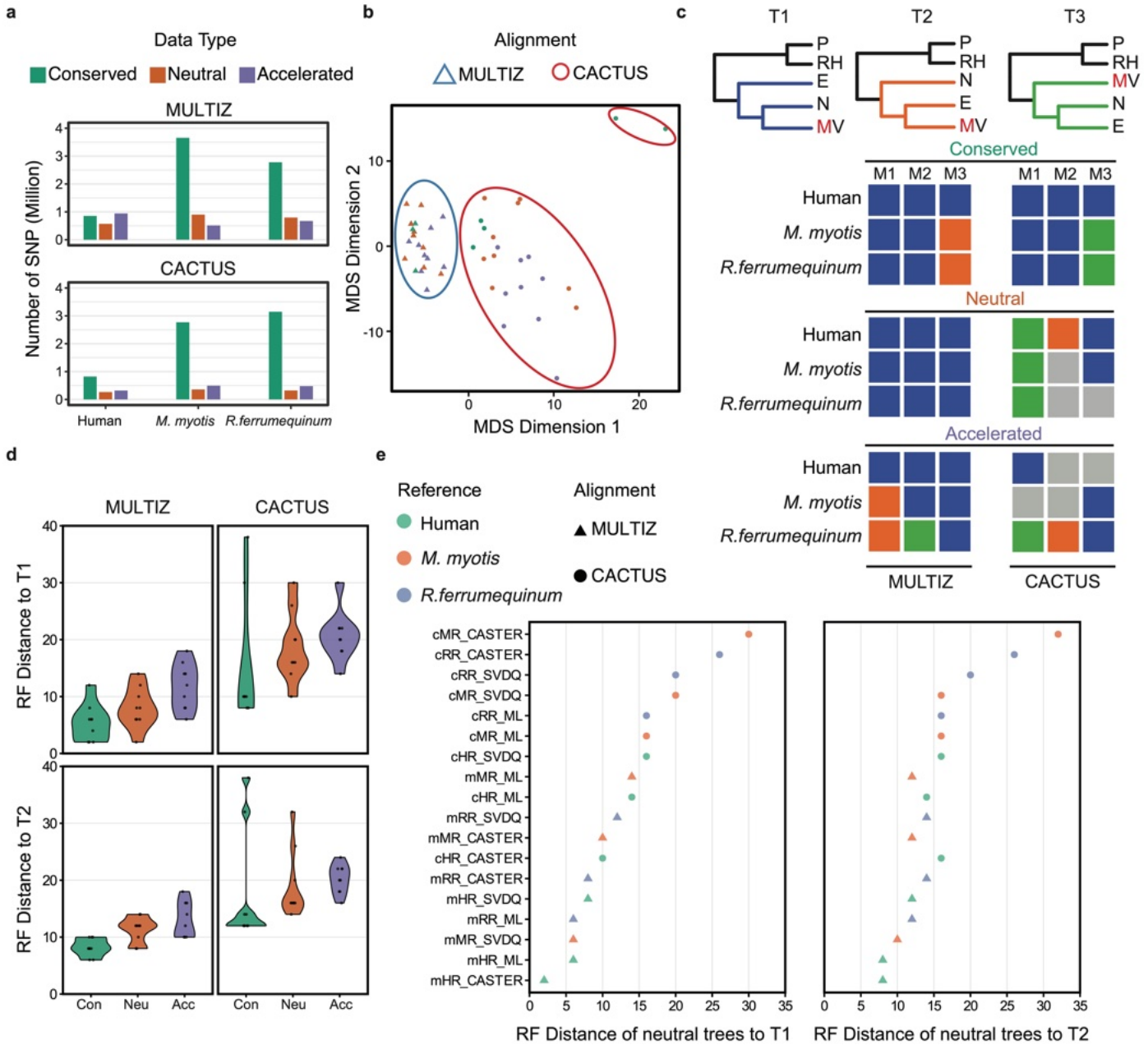

Extended Data Fig. 9 | Phylogenetic comparison of trees reconstructed from "dark genome". (**a**) Number of phyloP–based SNPs in subset–genome datasets across different alignments. (**b**) Multidimensional scaling (MDS) plot based on Robinson–Foulds distances among all the phylogenetic trees. (**c**) Summary of superfamily–level topologies across all the trees. P: Pteropodidae; RH: Rhinolophoidea; E: Emballonuroidea; N: Noctilionoidea; V: Vespertilionoidea. M1: Maximum likelihood; M2: SVDQuartets; M3: CASTER. Grey square: Other topologies. (**d**) Violin plot for the Robinson–Foulds distance of all the trees relative to the T1 and T2 topologies. RF, Robinson–Foulds; T1, protein-coding genes tree topology; T2, XLRD tree topology. Con, conserved; Neu, neutral; Acc, accelerated. (**e**) Dot plot for the Robinson–Foulds distance of all the neutral trees relative to T1 and T2 topologies. Alignments are abbreviated as mHR, mMR and mRR for MULTIZ *Homo sapiens*, *Myotis myotis* and *Rhinolophus ferrumequinum* references, respectively, and cHR, cMR and cRR for the corresponding CACTUS references. ML, maximum likelihood; SVDQ, SVDQuartets.

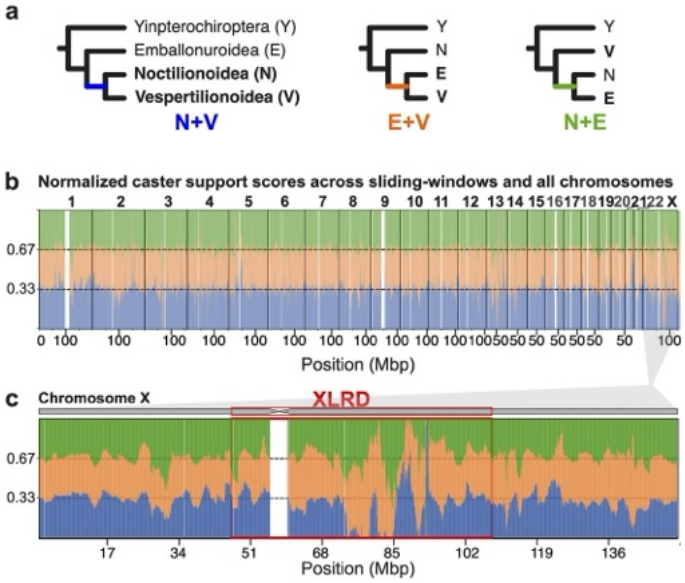

Extended Data Fig. 10 | Chromosomal landscape of phylogenetic support across yangochiropteran superfamilies reveals a diagnostic signal on the X chromosome and the X-linked Recombination Desert (XLRD)[38]. (**a**) Hypotheses tested for branch-specific support in CASTER analyses. (**b**) Normalized CASTER support scores for the branch highlighted in the three alternative topologies depicted in (a), averaged across 5-Mbp sliding windows for each chromosome. Windows lacking alignment coverage or with insufficient branch-specific information (for example, excessive gaps in the quartets) are left blank. (**c**) Zoomed view of the X chromosome highlighting the X-linked recombination desert (XLRD) spanning the interval between JADE3 and CHRDL1 (coordinates 47,061,242–110,673,856 in the MULTIZ-human reference genome).

Author Queries

Journal: **Nature**
Paper: **s41586-026-11007-3**
Title: **Reference genomes and fossils revise bat family phylogeny and biogeography**

AUTHOR:
The following queries have arisen during the editing of your manuscript. Please answer by making the requisite corrections directly in the e.proofing tool rather than marking them up on the PDF. This will ensure that your corrections are incorporated accurately and that your paper is published as quickly as possible.

Query Reference	Reference
Q1	A single sentence summarizing your paper has been provided (editor's summary in the eproof), which will appear online on the table of contents and in e-alerts. Please check this sentence for accuracy and appropriate emphasis.
Q2	Please carefully check that all credit lines have been correctly assigned.
Q3	Please check and confirm that the details for all affiliations are correct.
Q4	Your paper has been copy edited. (1) Please review every sentence to ensure that it conveys your intended meaning; if changes are required, please provide further clarification rather than reverting to the original text. Please note that formatting (including hyphenation, Latin words, and any reference citations that might be mistaken for exponents) and usage have been made consistent with our house style.(2) Check the title and the first paragraph with care, as they may have been re-written to aid accessibility for non-specialist readers.(3) Check the symbols for affiliations with care, and check all author names and Acknowledgements carefully to ensure that they are correct; check the email address of the corresponding author and the Competing Interests statement.(4) Check that there has been no corruption of mathematical symbols. Only single-letter variables are set in italics (but not their subscripts unless these are also variables); multi-letter variables are set in roman. Vectors are set as bold; matrices are set as italic only. We do not use italics for emphasis. Genetic material is set in italic and gene products are set upright. Please check that italicization and bolding are correct throughout. (5) Ensure that, where practicable, all figures, tables and other discrete elements of Supplementary Information are referred to at least once in the paper at an appropriate place in the text or figure legends.(6) Please note, we reserve 'significant' and its derivatives for statistical significance. Please reword where this is not the intended meaning (for example, to important, notable, substantial).
Q5	Please check that the display items are as follows (ms no: 2025-06-15921C): Figs 0 (black & white); 5 (colour); Tables: None; Boxes: None; Extended Data display items: 10 figures; SI (including reporting summary or peer review file): yes. The eproof contains the main-text figures edited by us and (if

Author Queries

Journal: **Nature**
Paper: **s41586-026-11007-3**
Title:**Reference genomes and fossils revise bat family phylogeny and biogeography**

AUTHOR:
The following queries have arisen during the editing of your manuscript. Please answer by making the requisite corrections directly in the e.proofing tool rather than marking them up on the PDF. This will ensure that your corrections are incorporated accurately and that your paper is published as quickly as possible.

Query Reference	Reference
	present) the Extended Data items (unedited except for minor formatting) and the Supplementary Information (unedited). Please check the edits to all main-text figures (and tables, if any) very carefully, and ensure that any error bars in the figures are defined in the figure legends. Extended Data items may be revised only if there are errors in the original submissions. If you need to revise any Extended Data items please upload these files when you submit your corrections to this eproof, and include a list of what has been changed.
Q6	Please note that affiliations have been reordered so that they are listed in numerical order. However, if it is important that the order of the affiliations is retained, we can split off the earlier affiliation by changing it slightly in comparison to the other affiliation, so that it is no longer identical, for example, by adding or removing a department or centre.
Q7	Please note, we reserve 'significant' and its derivatives for statistical significance. Please reword where this is not the intended meaning (for example, to important, notable, substantial).
Q8	Please note that we do not include a heading immediately after the abstract, therefore the heading was removed to comply with style.
Q9	Please provide the city for affiliations 41,75 and 77 where indicated and please check the city, state and country for affiliation 94.
Q10	Should affiliation 76 be split to comply with style as two universities are mentioned; note that style is to include one department, institution, city, state and country.
Q11	Please ensure that genes are correctly distinguished from gene products: for genes, official gene symbols (e.g., NCBI Gene) for the relevant species should be used and italicized; gene products such as proteins and noncoding RNAs should not be italicized.

Author Queries

Journal: **Nature**
Paper: **s41586-026-11007-3**
Title: **Reference genomes and fossils revise bat family phylogeny and biogeography**

AUTHOR:
The following queries have arisen during the editing of your manuscript. Please answer by making the requisite corrections directly in the e.proofing tool rather than marking them up on the PDF. This will ensure that your corrections are incorporated accurately and that your paper is published as quickly as possible.

Query Reference	Reference
Q12	Please check your article carefully, coordinate with any co-authors and enter all final edits clearly in the eproof, remembering to save frequently. Once corrections are submitted, we cannot routinely make further changes to the article.
Q13	Note that the eproof should be amended in only one browser window at any one time; otherwise changes will be overwritten.
Q14	Author surnames have been highlighted. Please check these carefully and adjust if the first name or surname is marked up incorrectly, as this will affect indexing of your article in public repositories such as PubMed. Also, carefully check the spelling and numbering of all author names and affiliations, and the corresponding author(s) email address(es). Please note that email addresses should only be included for designated corresponding authors, and you cannot change corresponding authors at this stage except to correct errors made during typesetting.
Q15	You cannot alter accepted Supplementary Information files except for critical changes to scientific content. If you do resupply any files, please also provide a brief (but complete) list of changes. If these are not considered scientific changes, any altered Supplementary files will not be used, only the originally accepted version will be published.
Q16	If applicable, please ensure that any accession codes and datasets whose DOIs or other identifiers are mentioned in the paper are scheduled for public release as soon as possible, we recommend within a few days of submitting your proof, and update the database record with publication details from this article once available.
Q17	(1) Please ensure that the following information is included in the figure legends where relevant. Sample size (exact n number); a statement of replicability (how many times was experiment replicated in the lab); description of sample collection (clarify whether technical or biological replicates and include

Author Queries

Journal: **Nature**
Paper: **s41586-026-11007-3**
Title:**Reference genomes and fossils revise bat family phylogeny and biogeography**

AUTHOR:
The following queries have arisen during the editing of your manuscript. Please answer by making the requisite corrections directly in the e.proofing tool rather than marking them up on the PDF. This will ensure that your corrections are incorporated accurately and that your paper is published as quickly as possible.

Query Reference	Reference
	how many animals, litters, cultures, etc.); state the statistical test used and give P values; define centre values (median or average) and error bars. (2) For figures/images that are reproduced or adapted from a third party, it is important that you confirm that permission has been obtained and that appropriate acknowledgement of the copyright holder is given. (3) Please note that we edit the main figures (but not the Extended Data figures) in house. There is no need to resupply any of the main figures to make minor changes to text labels to match the changes made in the text, as figures will have been edited accordingly. If you wish to make changes to any Extended Data figures, however, please resupply these, and please let us know what has changed.
Q18	Please check the panels and captions of all figures carefully, as these have been edited for style and clarity. Please make sure that any abbreviations listed only in the figure are defined in the caption.
Q19	In the sentence beginning "The numbers to the right of the scaffolds…", please define '/' and clarify throughout where necessary. Please note that we avoid the use of '/' to indicate interactions, alternatives, synonyms or complexes.
Q20	At the end of the caption for Fig. 5c, please define AU, EA, EF, EFA, FA, NEF, NE, NS and SU where indicated by ZZZ.
Q21	In Fig. 5, for the credit line "The 'Yango' silhouette was vectorized by A.E.M. from an illustration of *M. myotis* under a Creative Commons licence CC-BY-SA.", please indicate where the silhouette was vectorized from (e.g., Dinopedia, PhyloPic, etc).
Q22	Please clarify whether there is a difference between the grey and black text in Fig. 5c.

Author Queries

Journal: **Nature**
Paper: **s41586-026-11007-3**
Title: **Reference genomes and fossils revise bat family phylogeny and biogeography**

AUTHOR:
The following queries have arisen during the editing of your manuscript. Please answer by making the requisite corrections directly in the e.proofing tool rather than marking them up on the PDF. This will ensure that your corrections are incorporated accurately and that your paper is published as quickly as possible.

Query Reference	Reference
Q23	The acknowledgements have been edited for style and brevity; note, we do not include titles or affiliations and only include the initial(s) of the first name(s) of colleagues mentioned here. Please check.
Q24	In the Author contributions, please clarify how M.Hackenberg contributed to this work.
Q25	Please check that all funders have been appropriately acknowledged and that all grant numbers are correct.
Q26	If refs. 83 and 89 have now been published in peer-reviewed form, please update the references with the journal name, DOI (or volume and page numbers) and year of publication.

Emma C. Teeling,
Michael Hiller,
Liliana M. Dávalos,
Sonja C. Vernes,
David A. Ray

Corresponding author(s):

Last updated by author(s): 06/26/2026

Reporting Summary

Nature Portfolio wishes to improve the reproducibility of the work that we publish. This form provides structure for consistency and transparency in reporting. For further information on Nature Portfolio policies, see our Editorial Policies and the Editorial Policy Checklist.

Statistics

For all statistical analyses, confirm that the following items are present in the figure legend, table legend, main text, or Methods section.

n/a	Confirmed
☐	☒ The exact sample size (*n*) for each experimental group/condition, given as a discrete number and unit of measurement
☐	☒ A statement on whether measurements were taken from distinct samples or whether the same sample was measured repeatedly
☒	☐ The statistical test(s) used AND whether they are one- or two-sided *Only common tests should be described solely by name; describe more complex techniques in the Methods section.*
☒	☐ A description of all covariates tested
☐	☒ A description of any assumptions or corrections, such as tests of normality and adjustment for multiple comparisons
☐	☒ A full description of the statistical parameters including central tendency (e.g. means) or other basic estimates (e.g. regression coefficient) AND variation (e.g. standard deviation) or associated estimates of uncertainty (e.g. confidence intervals)
☐	☒ For null hypothesis testing, the test statistic (e.g. *F*, *t*, *r*) with confidence intervals, effect sizes, degrees of freedom and *P* value noted *Give P values as exact values whenever suitable.*
☐	☒ For Bayesian analysis, information on the choice of priors and Markov chain Monte Carlo settings
☒	☐ For hierarchical and complex designs, identification of the appropriate level for tests and full reporting of outcomes
☒	☐ Estimates of effect sizes (e.g. Cohen's *d*, Pearson's *r*), indicating how they were calculated

Our web collection on statistics for biologists contains articles on many of the points above.

Software and code

Policy information about availability of computer code

Data collection

Sequencing data were generated using standard commercial sequencing platforms, including PacBio Sequel II and Sequel IIe systems, Illumina NovaSeq 6000 and NextSeq 2000 instruments, and Oxford Nanopore PromethION. PacBio HiFi reads were generated using manufacturer-provided instrument control software, with CCS generated using the CCS tool (v6.0.0) within SMRT Link v10.1.0.119588. Details on kits, protocol versions, and sequencing instruments are provided in Supplementary Table 2.1. No custom software was used for sequencing data collection.

Data analysis

The following custom scripts used in this study are available at:
Transposable element annotation and curation (https://github.com/davidaray/Bat1k_TE_curation).
Sliding-window analysis (https://github.com/ariadnamorales/Bat1K_21Fam_Phylogenomics).
SNP2fasta extraction (https://gitlab.com/yan-liang/Bat1K_analysis/).
Nonindependent morphological characters analysis (https://github.com/lmdavalos/morpho_characters.)

In addition to custom scripts, the following publicly available software and pipelines were used for data analysis across different analytical sections. Detailed workflows and parameters are described in the Supplementary Notes 2-18.
Genome assembly and curation (PacBio ccs v4.2.0–6.4.0, DeepConsensus v0.2.0–1.2.0, blastn (v.2.13.0), hifiasm v0.13–0.19, Falcon assembler (v1.8.1),MARVEL assembler , DAmar pipeline v1 (https://github.com/MartinPippel/DAmar), Foreign Contamination Screen Tool (FCS, v0.5.0), BlobTools v4.1.0, purge-dups (v.1.2.6), gcpp (https://github.com/PacificBiosciences/gcpp),
pbmm2 (v.1.7.0) , minimap (v2.24-2.28),
deepvariant (v1.2.0), picard (v.2.26.10), bcftools (v.1.16), Daccord (https://github.com/gt1/daccord), FreeBayes v1.3.6 (https://github.com/

freebayes/freebayes/), PEPPER-Margin-DeepVariant
v0.8 (https://github.com/kishwarshafin/pepper), Merfin v1.1 (https://github.com/arangrhie/merfin), Falcon v1.8.1, SALSA2 v2.2–2.3, YaHS v1.1, bwa (v0.7.17), chromap (v0.2.5-0.2.6),
paritools (v0.3.0), mitohifi (v2.0-2.2),
Juicebox (v1.11.08), PretextView (v.0.2.5) and HighGlass (v.0.4.17).).
Genome statistics and completeness assessment (TOGA v1, compleasm v0.2.7 with mammalia_odb12,Merqury v1.0).
Protein-coding gene annotation and orthology inference (RepeatMasker v4.0.9, RepeatModeler(http://www.repeatmasker.org/, parameter -engine NCBI), LASTZ v1.04.15, RepeatFiller v1.0, TOGA (https://github.com/hillerlab/TOGA, commit v.c4bce48), GENCODE v38 and Ensembl 104, human reference genome hg38 (GRCh38.p12)).
Transposable element annotation (HiTE v3.1.2; RepBase RepBaseRepeatMaskerEdition-20181026, TEClass2 (https://www.bioinformatics.uni-muenster.de/tools/teclass2/index.pl?lang=en), Usearch v11.0.667, TEAid v1.0.0).
Exploration between genome assembly size and TE proportion (brms v. 2.23.0. ggplot2 v. 4.0.3, scales 1.4.0, tidybayes v. 3.0.7, magrittr v. 2.0.5, and ggthemes v. 5.2.0.)
MicroRNA annotation (MirMachine v0.3.0, phytools v2.5-2, DOLLOP v3.5c,R v4.5.1).
Whole-genome alignments (MULTIZ v11.2, LASTZ v1.04.15, Progressive Cactus v2.6.13, halValidate v2.2, hal2maf v2.9.2, maftools v0.1, PHAST v1.5, R v4.4.1, NetFilterNonNested.perl (https://github.com/hillerlab/GenomeAlignmentTools), mafAddIRows (https://github.com/ucscGenomeBrowser/kent),cactus-hal2maf (v2.9.2)).
Protein-coding gene phylogenetic analyses (MACSE v2, HmmCleaner v0.180750, RAxML v8.1.16, ASTRAL v5.5.9, BOOSTER v1, PHAST v1.5, CASTER v1.19.1.4, MonoPhy v1.3.1, ape v5.7-1 in R v4.2.0).
Concatenated phylogenetic analyses (FASconCAT-G v1.06, IQ-TREE2 v2.1.3,phangorn v2.10.0, R (v4.2.2),ASTRAL (v5.5.7), Weighted ASTRAL (v1.24.3.8), GoTree (v0.5.1-12)).
Gene concordance analyses (Newick Utilities, https://github.com/tjunier/newick_utils; IQ-TREE3 v3.0.0).
Dark SNP-based phylogenetic analyses (cactus v2.8.2, PHAST v1.4–1.5, SNP-sites v2.5, bedtools v2.31.1, IQ-TREE2 v2.3.4, PAUP* v4.0a169-c1, aster v1.1.9-c3, pheatmap v1.0.13, ggplot2 v4.0.1, ape v5.8.1, phytools v2.5.2, R v4.5).
X-linked reduced-recombination domain (XLRD) analyses (PHAST v1.4–1.5, SNP-sites v2.5, bedtools v2.31.1, IQ-TREE2 v2.3.4, CASTER v1.19.1.4, ape v5.8.1, phytools v2.5.2, R v4.5).
Mitochondrial phylogenetic analyses (MitoHiFi v3.2.2, BLAST+, MitoFinder v1.4, MAFFT v7.525, Gblocks v0.91b, IQ-TREE v2.3.4, FigTree v1.3.1).
Ancestral karyotype reconstruction (DESCHRAMBLER, SyntenyPlotterR v1.0.0,R v. 4.3, BUSCO v 4. 0. 4.0.5 (mammalian OrthoDB v. 10 dataset)).
Divergence time estimation and fossil-based dating (mcmctree v4.9e, RAxML v8.2.12, PHAST v1.4, RevBayes v1.2.2, ape v5.8.1, phytools v2.0, R v4.2.1,PAML suite (v4.9d)).
Biogeographic analyses (RevBayes v1.2.2, RevGadgets v1.2.1, ape v5.8.1, treeio v1.20.2, ggtree v3.4.4, R v4.2.1).

For manuscripts utilizing custom algorithms or software that are central to the research but not yet described in published literature, software must be made available to editors and reviewers. We strongly encourage code deposition in a community repository (e.g. GitHub). See the Nature Portfolio guidelines for submitting code & software for further information.

Data

Policy information about availability of data

All manuscripts must include a data availability statement. This statement should provide the following information, where applicable:

- Accession codes, unique identifiers, or web links for publicly available datasets
- A description of any restrictions on data availability
- For clinical datasets or third party data, please ensure that the statement adheres to our policy

Newly generated genome assemblies have been deposited in the European Nucleotide Archive (ENA) under the Bat1K project (https://www.ncbi.nlm.nih.gov/bioproject/489245), with associated raw sequencing data linked through the corresponding ENA records. Accession information for both newly generated and previously published datasets used in this study is summarized in Supplementary Table 1.1.
Processed data supporting the findings of this study are available from Dryad at: DOI: 10.5061/dryad.1rn8pk187
The codes of this study are available at:
https://github.com/Bat1K-21families/21families-analyses
There are no restrictions on data availability.

Research involving human participants, their data, or biological material

Policy information about studies with human participants or human data. See also policy information about sex, gender (identity/presentation), and sexual orientation and race, ethnicity and racism.

Reporting on sex and gender	The study does not involve human participants,biological material and data.
Reporting on race, ethnicity, or other socially relevant groupings	The study does not involve human participants, biological material and data.
Population characteristics	The study does not involve human participants, biological material and data.
Recruitment	The study does not involve human participants, biological material and data.
Ethics oversight	The study does not involve human participants, biological material and data.

Note that full information on the approval of the study protocol must also be provided in the manuscript.

Field-specific reporting

Please select the one below that is the best fit for your research. If you are not sure, read the appropriate sections before making your selection.

☐ Life sciences ☐ Behavioural & social sciences ☒ Ecological, evolutionary & environmental sciences

For a reference copy of the document with all sections, see nature.com/documents/nr-reporting-summary-flat.pdf

Ecological, evolutionary & environmental sciences study design

All studies must disclose on these points even when the disclosure is negative.

Study description	This study aimed to investigate the family-level phylogeny and deep evolutionary history in bats. We generated and analysed chromosome-level referenced genome assemblies, performed whole-genome annotation, and inferred phylogenetic relationships using multiple genome-wide data partitions. Comprehensive evolutionary analyses were conducted to reconstruct ancestral karyotypes, estimate divergence times using molecular and fossil data, and infer global biogeography.
Research sample	Genome assemblies from 103 bat species representing all extant 21 bat families were included in this study. Of the 103 species genomes, 43 reference-quality genomes belonging to 42 distinct bat species (for Hipposideros caffer, we sequenced two separate subspecies) are newly presented in this study, and genomes for 61 species were already sequenced under the Bat1K umbrella. Details of the published assemblies are listed in Supplementary Table 1.1.
Sampling strategy	Species were selected to cover all extant 21 bat families in Chiroptera.
Data collection	For seven of the 43 new genomes, we generated PacBio continuous long reads (CLR), 10X Illumina read-cloud data, and Bionano optical maps. For 34 genomes, We sequenced PacBio high fidelity (HiFi) reads. For the New Zealand-endemic Mystacina tuberculata, we generated Oxford Nanopore long read data and 10X Illumina read-cloud data. For all 43 genomes, we generated HiC data for scaffolding. Information on data collection procedures is provided in Supplementary Table 2.1.
Timing and spatial scale	Bat species used for genomic sequencing were generated over multiple years across a range of global, regional, and local geographic scales. Information on collection dates and locations is listed in Supplementary Table 1.1.
Data exclusions	The ONT-based assembly of Lyroderma lyra was excluded due to an excessive number of base errors. For protein-coding gene phylogenies, sequences of genes with missing or multiple co-orthologs in a given species were excluded from alignments. For sliding-window and neutral intergenic window phylogenies, alignments with <80% species coverage were excluded.
Reproducibility	Analyses are reproducible using the provided data and the software described in the Methods.
Randomization	Null expectations for neutral intergenic window analyses were generated using 100 randomized datasets for the human-referenced alignment, preserving window size and alignment constraints. To decrease the computation time for analyses of fossilized birth–death (FBD) models, 10,000 sites were randomly sampled from 92,048 neutral sites.
Blinding	All groupings were produced through bioinformatic cutoffs; therefore blinding was not relevant.

Did the study involve field work? ☐ Yes ☒ No

Reporting for specific materials, systems and methods

We require information from authors about some types of materials, experimental systems and methods used in many studies. Here, indicate whether each material, system or method listed is relevant to your study. If you are not sure if a list item applies to your research, read the appropriate section before selecting a response.

Materials & experimental systems

n/a	Involved in the study
☒	☐ Antibodies
☒	☐ Eukaryotic cell lines
☐	☒ Palaeontology and archaeology
☐	☒ Animals and other organisms
☒	☐ Clinical data
☒	☐ Dual use research of concern
☒	☐ Plants

Methods

n/a	Involved in the study
☒	☐ ChIP-seq
☒	☐ Flow cytometry
☒	☐ MRI-based neuroimaging

Palaeontology and Archaeology

Specimen provenance	For total evidence dating we used fossil information from 34 species of our 44 fossil taxa, representing 17 extant and 10 extinct families, with 6 species unassigned to extinct families. Full details on geographic localities, age range, and character completeness required are provided in Supplementary Section 16 and Supplementary Table 16.1.
Specimen deposition	Fossil data were compiled from published sources, as detailed in Supplementary Table 16.1.
Dating methods	Fossil range was compiled from published sources, detailed in Supplementary Table 16.1.

☒ Tick this box to confirm that the raw and calibrated dates are available in the paper or in Supplementary Information.

Ethics oversight	All fossil data used in this study were obtained from published sources; therefore, ethical approval was not required.

Note that full information on the approval of the study protocol must also be provided in the manuscript.

Animals and other research organisms

Policy information about studies involving animals; ARRIVE guidelines recommended for reporting animal research, and Sex and Gender in Research

Laboratory animals	Of the 43 newly reported genome assemblies, representing 42 species, only one species, Leptonycteris yerbabuenae, was collected from a captive colony maintained at the University of Tübingen, which was established before 2014.
Wild animals	Of the 43 newly reported genome assemblies, samples representing 41 species were obtained from wild animals captured in the field under appropriate local permits. Species information is provided in Supplementary Table 1.1.
Reporting on sex	Samples included both male and female individuals across species. Sex was not a factor in the study design. Each species was represented by one sex only, as detailed in Supplementary Table 1.1.
Field-collected samples	Field-collected samples were collected for tissue dissection and were not maintained in the laboratory for long-term captivity. All procedures were conducted under appropriate local permits. Detailed permit information, including issuing bodies and permit numbers, is provided in Supplementary Table 1.1.
Ethics oversight	All field collections were carried out under appropriate local permits granted by national or regional environmental and wildlife agencies. Detailed permit information, including issuing bodies and permit numbers, is provided in Supplementary Table 1.1.

Note that full information on the approval of the study protocol must also be provided in the manuscript.

Plants

Seed stocks	Not applicable.
Novel plant genotypes	Not applicable.
Authentication	Not applicable.